

tonous structure which corresponds to the thick and wide Trusmadi Formation consisting of sandstone and mudstone.

Section F

This is a NE-SW section passing through the western side of "b" area. Near Nos. 25–27, the high resistivity from the surface suggests a thick peridotite body. On both sides of the resistive zone, it is interpreted a vertical fault structure showing a high contrast. The low resistivity of less than 50 ohm-m may reflect the Trusmadi formation, as is the case of the Section E.

Section G

This line, parallel to the Section F, passes through the eastern side of the "b" area. Around Nos. 199–8, there are, unlike the case of the Sections E and F, distributed peridotite which shows two-layer structure of high over low (50–70 ohm-m) at depths. The low resistivity detected in the peridotite may be attributed to the fact that the rock has a strong argillization at depths.

3-2-3 Resistivity Structural Map

Resistivities at the depths of 50 m, 150 m and 200 m below ground surface, derived from the results of 1-D inversion analysis and 2-D model analysis, were chosen and three kinds of resistivity structural maps were made as shown in Figs 73–75 and Maps 54–56.

(1) As three maps show a common feature, an uniform underground structure from ground surface to 200 m depth is assumed in the area.

(2) Two high resistivity zones of more than 100 ohm-m are distributed in the following two areas:

1) This zone is located at the northwestern portion of the area, and shows a common feature on each map so the causative rock and/or layer may be compact.

2) This zone is located at the central portion and extends to northwestern direction. Resistivities in the zone increase with depth so it is thought that the causative body may be more compact at depths. And on the map of 200 m depth, the zone extends to the south so that the causative body may exist in the southern side in depths.

The zone is divided into several blocks and fault structures are assumed. And at the both sides of the zone large faults structures may exist.

This high resistivity zone may be caused by outcropping peridotite.

(3) Low resistivity zones are distributed in the northeastern, central, southwestern and northern portions and show a common feature at each depth.

These may correspond to Trusmadi Formation mainly consisted of sandstone, but the

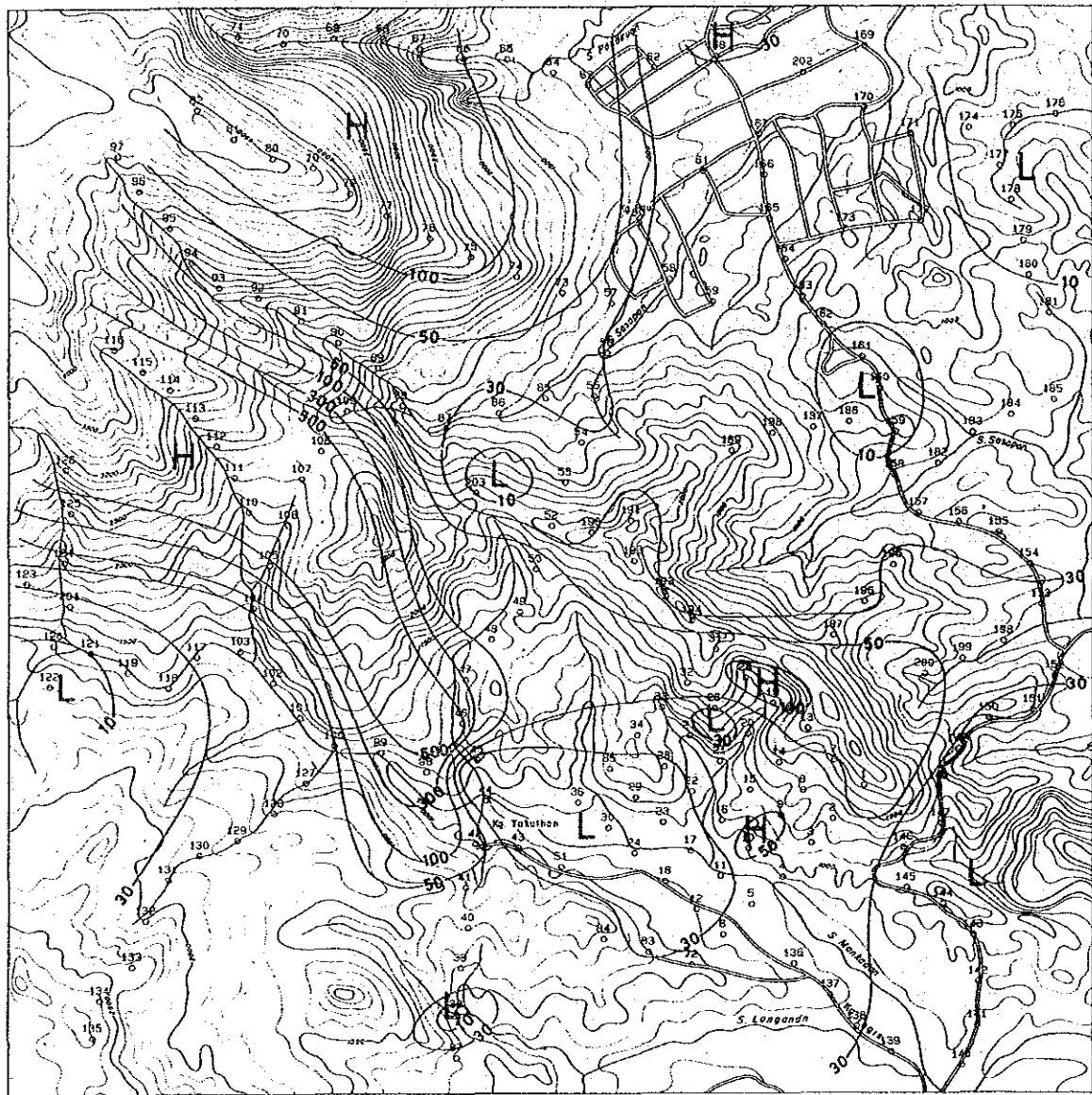


Fig. 73 Resistivity Structural Map in "B" Area (50m)

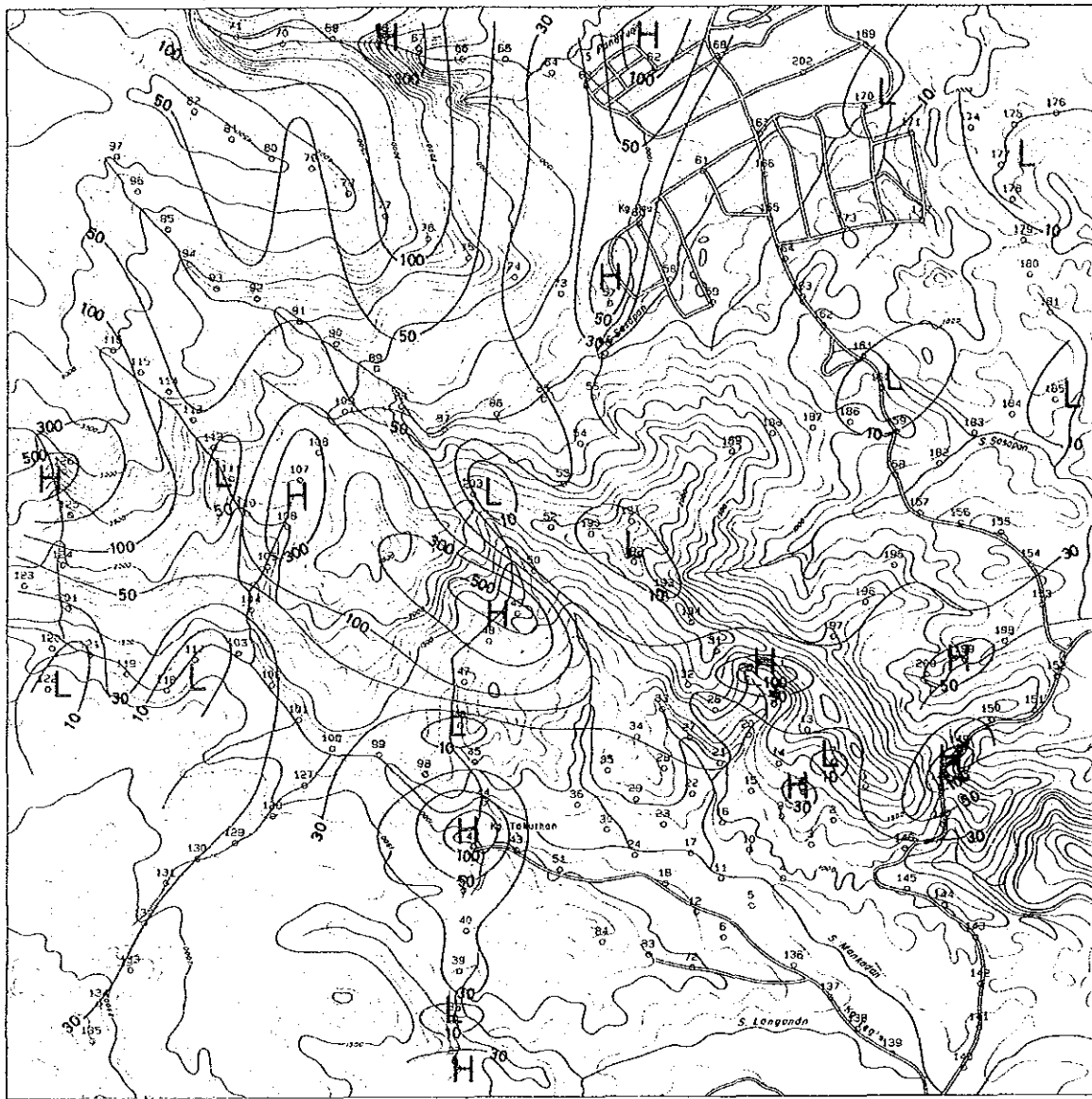


Fig. 74 Resistivity Structural Map in "B" Area (150m)

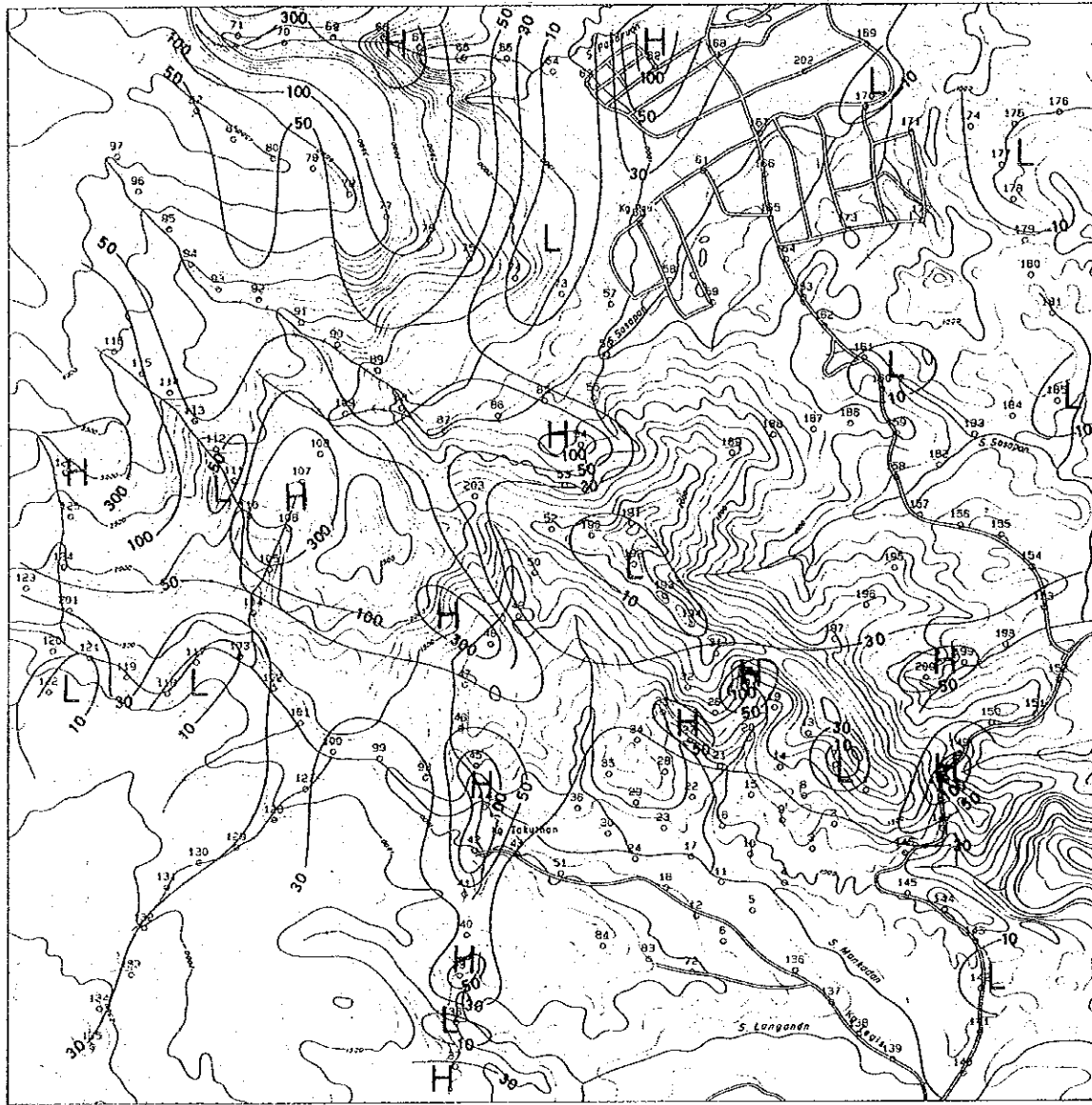


Fig. 75 Resistivity Structural Map in "B" Area (200m)

northern one extending to NS direction may be caused by NS striking fault structure.

3-2-4 Resistivity Section

Based on the results of 1-D inversion analysis of each station, 2-D model analysis were made for selected three sections, E, F and G, and the results are shown in Figs. 76-78.

On three sections, resistivity structure suggesting a simple geological structure except for small area "D" can be seen.

(1) Section E

A complex structure of more than three layers is found on the section except for the south of No. 41.

At the south of No. 41, resistivity and thickness of the first layer are 60-80 ohm-m and 20-30 m, respectively and resistivity of the second layer is of less than 50 ohm-m. One layer of thickness of about 40 m suggesting of less than 50 ohm-m which may be caused by fracture zone, is found beneath a highly resistive rock. The first and second layers at the south of No. 41 may correspond to volcanic rock and Trusmadi Formation, respectively.

A resistivity layer which may be caused by Trusmadi Formation is widely distributed on the whole section.

Between Nos. 42 and 48, a structure consists of four layers (low-high-low-high) and in depths a high resistivity of more than 100 ohm-m layer suggesting a dome-like structure is found. A resistivity layer of less than 10 ohm-m with thickness of 100 m between Nos. 44 and 46 does not extend to NS direction so it may be a local low-resistivity one.

Between Nos. 47 and 50, resistivities of the first and second layers are of 50-85 ohm-m and of more than 100 ohm-m, respectively. Resistivity of the third layer is different from each other at the both sides of a resistivity discontinuity line assumed between Nos. 48 and 49; of more than 30 ohm-m on the southern side and of less than 30 ohm-m on the northern side.

Between Nos. 52 and 54, there is no layer corresponding to the first layer Nos. 47-50. Resistivity and thickness of the second layer are of 30 ohm-m and 300 m, respectively, and this layer extends from No. 49. This layer is thickly distributed below 20 m depth at No. 56 and below 200 m depth at the north of No. 57. The first layer with thickness of 30 m may correspond to peridotite because this rock is distributed between Nos. 52 and 54.

The second and/or third layers with resistivity of 30-50 ohm-m may correspond to Trusmadi Formation, which may be divided into two, based on resistivity, that is, 30-50 ohm-m to mainly sandstone and 50-100 ohm-m to mudstone.

On the section, many resistivity discontinuity lines are assumed and resistivity structure is

divided into many small blocks. Remarkable fault structures are found at No. 38, 41–42, 46–47, 48–49, 50–52 and 54–55.

(2) Section F

Two-layer structure is found on the section except for Nos. 27–25 where a complex structure is assumed.

Between Nos. 39 and 28, the first layer is different from each other at the both sides of No. 30 where a fault structure is found. Between Nos. 39 and 30, the first layer shows a resistivity of about 100ohm-m and its thickness is about 20 m but it decreases its thickness toward south and there can not be seen the first layer at No. 39. On the other hand, between Nos. 30 and 28, this first layer shows a resistivity of about 45ohm-m and a thickness of 50 m at Nos. 29–27, but it decreases its thickness abruptly near a fault structure at No. 30.

At the south of No. 28, as the second layer of resistivity of less than 30ohm-m is distributed thickly and the resistivity change of within this layer is very little, this layer may reflect a uniform geology.

The first layer between Nos. 39 and 30 and the second layer between Nos. 39 and 28 may correspond to igneous rock and sandstone of Trusmadi Formation, respectively.

Between Nos. 27 and 25, peridotite is distributed and many faults are inferred so in this part it is thought that many fractures are developed and groundwater and/or clay fulfill these fractures. A low resistivity layer below No. 26 may reflect these conditions. Judging from geological condition and resistivity structure, peridotite is not distributed thickly and another highly resistive rock with the same resistivity may exist below this peridotite.

Between Nos. 197 and 185, resistivity of the first layer shows a lateral change of less than 50ohm-m and more than 50ohm-m. In this part, there is no geological information, but judging from the resistivity structure this layer is the same as that on the south of No. 27, and parts of resistivity of less than 50ohm-m may correspond to Trusmadi Formation. Higher resistivity parts of the layer may reflect local highly-resistive rocks (basalt).

(3) Section G

A resistivity structure is different from each other at the both sides of a resistivity discontinuity line assumed at Nos. 8–9.

At the southern side of Nos. 8–9 (i.e. Nos. 38–9), two-layer structure is assumed. The first layer of resistivity of more than 50ohm-m shows its thickness of 30 m at Nos. 11–83 and 70 m at No. 9 and increases its thickness toward south. The second layer of resistivity of less than 30ohm-m is distributed thickly. The first layer may correspond to andesitic lava which shows a sheet-like distribution and the second layer to Trusmadi Formation composed mainly of sand-

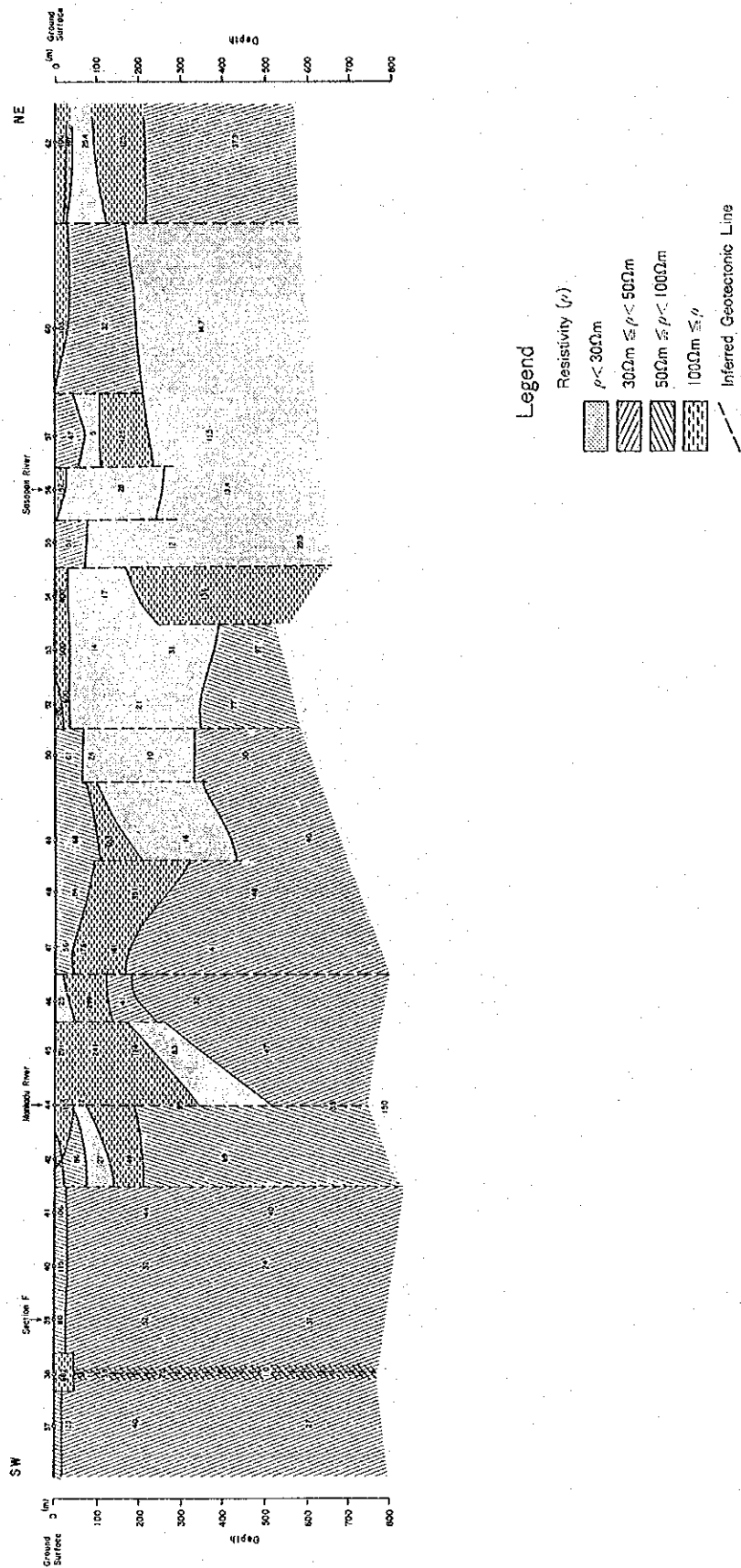


Fig. 76 Resistivity Section in "B" Area (Section E)

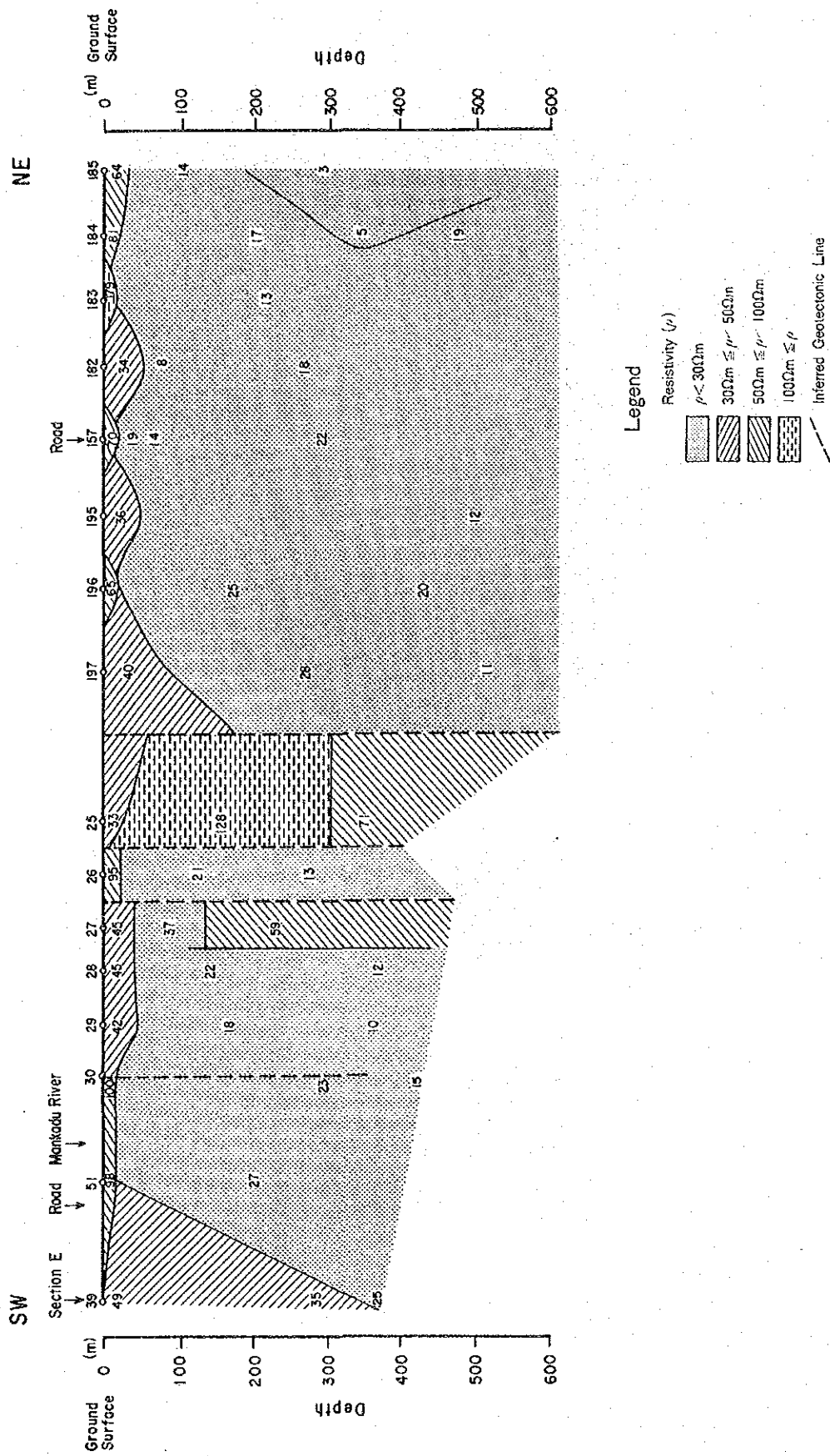


Fig. 77 Resistivity Section in "B" Area (Section F)

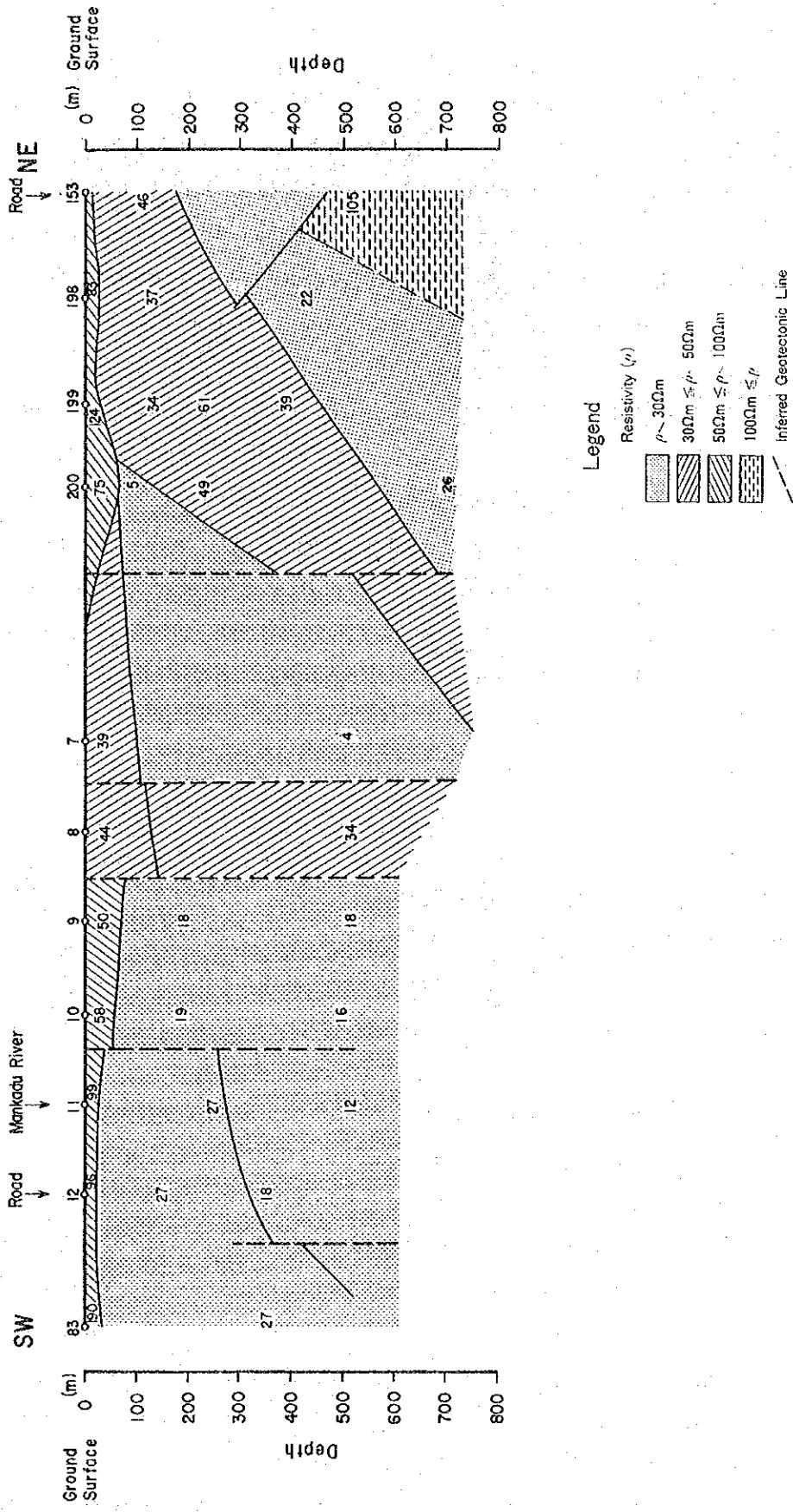


Fig. 78 Resistivity Section in "B" Area (Section G)

stone and mudstone.

On the other hand, on the northern side (Nos. 8–153) of Nos. 8–9, a three-layer structure is found. The first layer of resistivity of 30–50ohm-m between Nos. 8–200 shows a thickness of more than 100 m and may correspond to the same geology as that of the second layer of Nos. 200–153. The second layer shows a resistivity of less than 30ohm-m and in particular very low resistivity of less than 5ohm-m at Nos. 7–200. This very low resistivity seems to be a local resistivity drop caused by low resistivity layer near ground surface and fracture zone associated with inferred faults at Nos. 8–7 and Nos. 7–200.

Between Nos. 200–153, the first layer of resistivity of more than 70 ohm-m shows a thickness of 70 m at No. 200 and 30 m at Nos. 199–153 and may reflect peridotite. Resistivity change within peridotite is very large so it is thought that peridotite is serpentinized and brecciated. In this part, lower layers from the second layer may correspond to Trusmadi Formation, but resistivity of the second layer is a little higher than that of the third so it may be possible to divide this formation into two; the second layer at Nos. 83–7 and the third layer at Nos. 200–153 may reflect sandstone of this formation, and the second layer at Nos. 200–153 may correspond to mudstone of this formation.

A high resistivity block is found at depth of 500 m below No. 153.

3–3 Discussion

This area B shows almost the same resistivity feature as the area A, with two resistivity areas due to peridotite. The one detected in the northwestern part of the area is considered to be due to massive and compact rock. The other, detected in the center of the area, may be caused by peridotite splitted into several blocks by a N-S trending structural control, showing a NW-SE distribution.

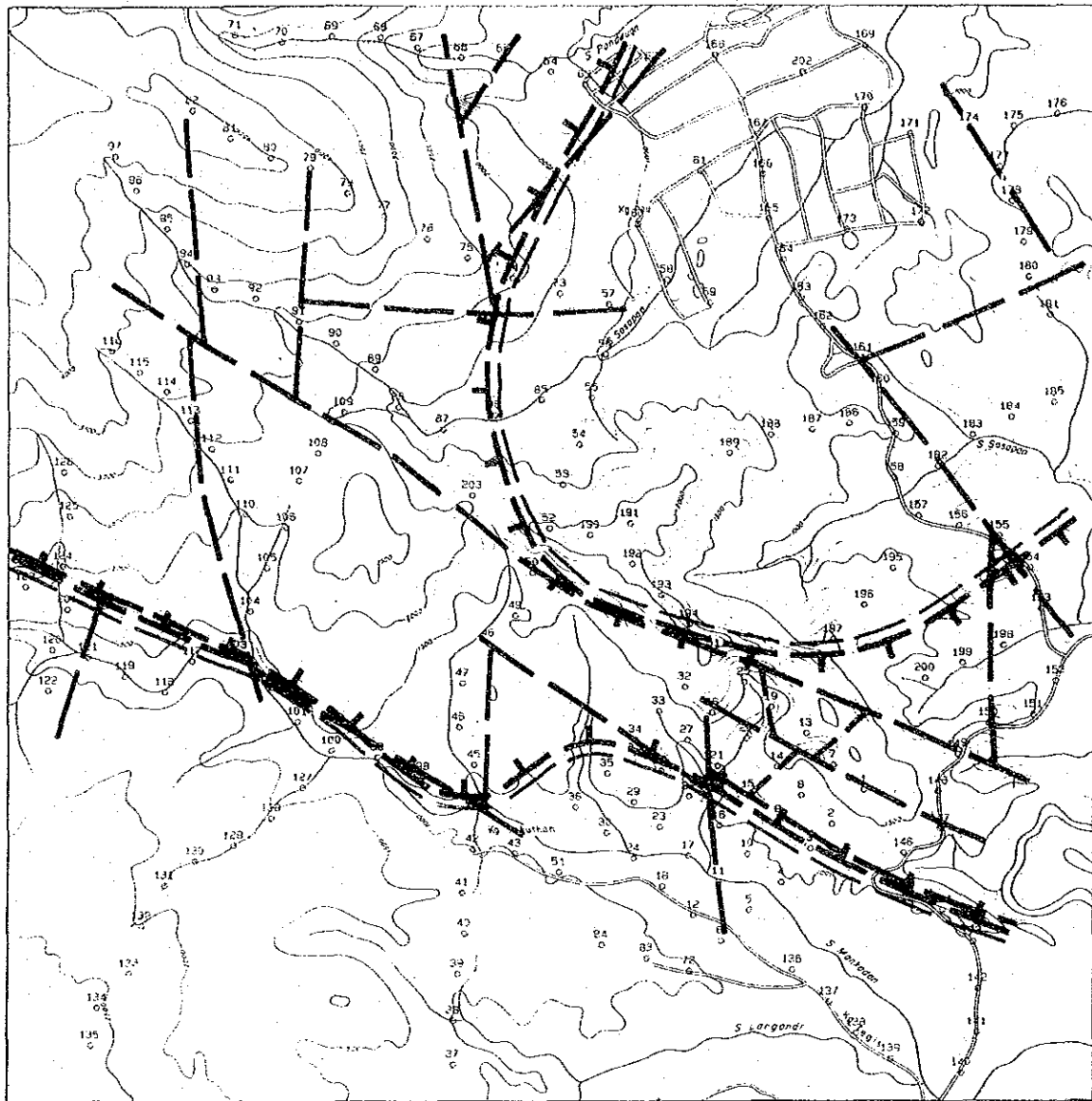
A strong argillization must be accompanied by the fault zone, however, there exist the possibility that this argillization might be caused by mineralization.

On the other hand, the resistivity zones of around the 30ohm-m are seen in the northwestern end of the area with a strong contrast. It is rather complicated to judge only from the CSAMT technique whether it is only caused by argillization or by mineralization.

Other low resistivity zones aside from the mentioned above, seems to correspond with the Trusmadi formations, which is widely and thickly distributed in the eastern area.

The interpreted resistivity zone which seems to be connected with mineralization in the area is the NW-SE trending high resistivity zone with a strong resistivity contrast.

In order to confirm the existence of sulfide minerals, it is strongly recommended to carry out the geophysical surveys with IP and SIP methods.



LEGEND

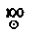



- 
Station and No.
- 
Line of Discontinuity
- 
High Resistivity Zone
- 
Resistivity Contour
(Dip 150m)

Fig. 79 CSAMT Interpretation Map in "B" Area

Chapter 4 Overall Discussion

This area has been drawn the attention for several decades as having a high potential for mineral resources because of the floats of high grade massive copper sulfide in the Lingangaa Creek, a branch of the Mankadau River, and massive chromite deposit near the boundary of peridotite in Paranchangan to the east of b area.

The geology of the area consists of sedimentary rocks (mainly sandstone) and peridotite which enplaces in the northeastern part of the area and is in a steep fault contact with the sedimentary rocks. On the northern side of the peridotite, spilitic basalt lavas are distributed, forming a mountain ridge, and shows also a sharp fault contact.

The sedimentary rocks have some characteristics of the Trusmadi Formation in some parts, however it should be correlated to the Chert-Spilitic Formation which was described in the area of Bidu-Bidu Hill, Lubuk Valley by Newton-Smith (1967).

The peridotite is correlated to "the Cretaceous and Tertiary ophiolitic intrusive rocks (Kirk, 1968)" and forms a part of the belt (25 miles wide) extending from Darvel Bay to Northern Islands via Segama Valley, Labuk Valley and Kinabaru.

Under the microscope, a colloform texture can be recognized in a part of massive sulfide ore, suggesting that the copper deposit is of a Cyprus type associated with ophiolite.

Coleman R. G. (1978) illustrated a ophiolite sequence in the Troodos deposits in Cyprus as plutonic complex (Harzburgite) → gabbro → sheeted intrusive complex → pillow lava (corresponding to the Chert - Spilitic Formation) → ore deposits → sedimentary rocks in an ascending order. When this is the same case, the source of floats seems to be at the same horizon as the spilitic basalt lava which is distributed on the ridge.

Any source outcrops could not be found by the geological survey which covered 4 km², centering around the ore floats but geochemical anomalies detected near the boundary between peridotite and basalt seems to be worth to check from a geological point of view, though the anomalous values are not so high.

Based on the result of CSAMT survey in the B area, a resistivity zone with more than 100 Ωm extends in a NW-SE direction, being well configured to the distribution of peridotite. As the above-mentioned floats of massive copper sulfide ore and chromite ore in the Lingangaa Creek and copper oxide ore in the Sansogo Creek (outside b area) and geochemical anomalies in soil or stream sediment are distributed in this zone, it is necessary to clarify the distribution, and geological structures of peridotite and Chert-Spilitic Formation and to elucidate the related mineralization.

PART IV c(PALIU) AREA

Chapter 1 Geology and Mineralization

1-1 Geology

1-1-1 Sedimentary Rocks

The sedimentary rocks in the Area are correlated to the Trusmadi Formation. Present data indicate however that the rock facies between Trusmadi Formation and Crocker Formation are rather similar and the relationship between the upper part of the former and the lower part of the latter is a lateral facies change. In addition to this, the red shale layer is interbedded in this sedimentary rock. Therefore there are some possibilities that the sedimentary group belongs to Crocker Formation.

Geological map, generalized stratigraphic section and columnar sections are shown in Figs. 16, 17 and 18 respectively.

The sedimentary rocks in this area are composed mainly of sandstone, interbedded with thin beds (about 10 to 30 m thick) of mudstone and shale. Sandstone beds may reach a total thickness of 500 m in southeastern part of the Area. The sedimentary rocks are divided into three facies based on the stratigraphy. They are in ascending order:

1. horizon of sandstone only,
2. horizon of sandstone intercalated with mudstone beds and
3. horizon of sandstone intercalated with shale bed.

In general the distribution of these three horizons is as follows: the lowest is in the northern part, the middle in the central part and the uppermost in the southeastern part. However it is very difficult to determine clearly the boundaries between these horizons.

The characteristics of rock facies are as follows:

(1) Sandstone facies

This sandstone is medium to fine grained, pale grey to grey colored, poorly-bedded, massive and hard, and locally grades into siltstone. This sandstone is often intercalated with thin mudstone layers with thickness of a few centimetres to several centimetres. They sometimes show rythmical alternating beds, and the ratio between sandstone and mudstone varies locally.

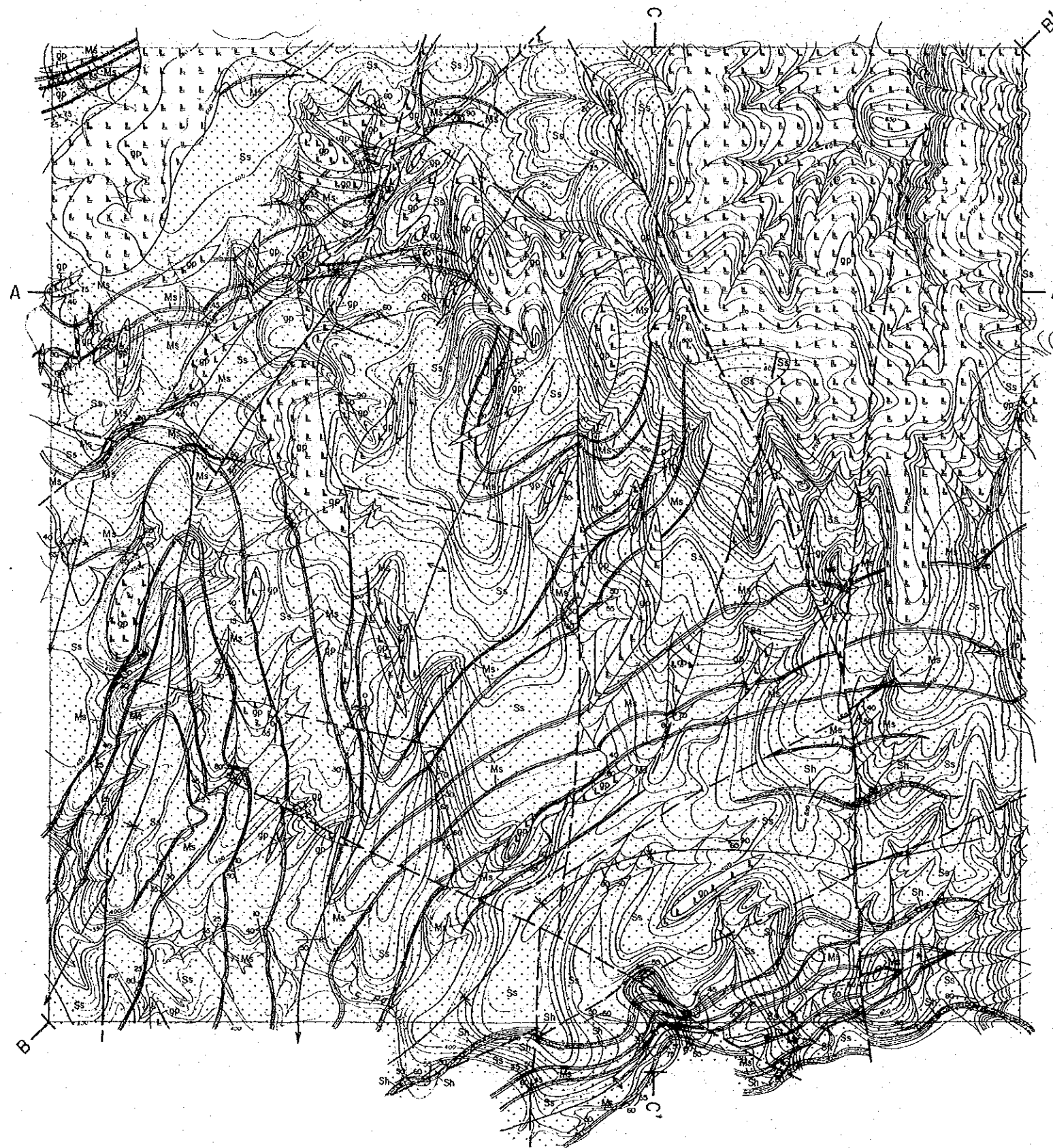
Sandstone metamorphosed to hornfels is observed around the contact zones with intrusive granodiorite porphyry bodies.

The characteristics of representative samples for microscopic study are described as follows;

T-07 Medium to fine grained sandstone

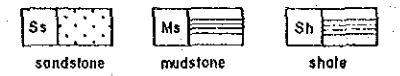
Grains : quartz > chert fragments > plagioclase, K-feldspar, muscovite, opaque minerals.

Characteristics : Sandstone medium (less than 0.3 mm) to fine grained; has a considerable



LEGEND

Trusmadi Formation



Intrusive Rock

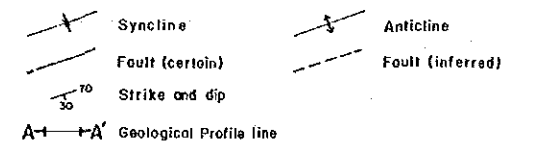
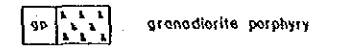


Fig. 80 Geological Map of "c" Area

matrix. Grain shape varies from subangular to subrounded, not well sorted and graded. Chlorite and sericite are observed as secondary minerals.

Y-05 Medium grained sandstone

Grains : quartz > chert fragments, plagioclase > K-feldspar, muscovite, opaque minerals

Characteristics : Arkose; bearing quartz, chert fragments and plagioclase. Grains mainly subangular (some subrounded), grain size is around 0.4 mm. The matrix consists of very fine grained quartz and sericite occurring as secondary minerals.

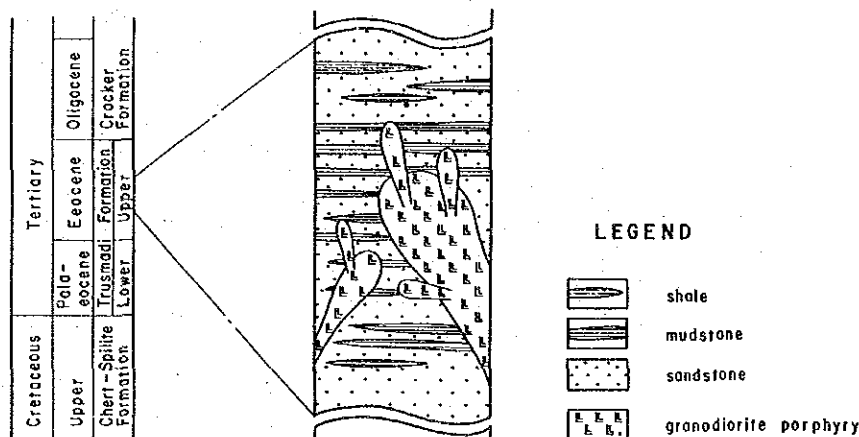
Siltstone facies show dark grey color and is rather well bedded. This layer is the product of gradual gradation from the sandstone and is widely distributed.

The results of microscopic study of the representative sample is as follows;

Y-18 Siltstone

Grains : quartz, opaque minerals

Characteristics : Mainly consists of quartz grain with size of 0.015 mm. Opaque minerals are also common. Matrix is so fine that mineral assemblage can not be identified. There are some stringers in specimen which consists of quartz and zeolite. Sericite is a secondary mineral.



note) Granodiorite porphyry is supposed to be intruded in Late Pliocene age.

Fig. 81 Generalized Stratigraphic Section of "c" Area

2) Mudstone facies

This rock is interbedded with sandstone and is dark grey to black, colour and well-bedded. The mudstone is well exposed laterally, but in some parts is intercalated with thin layers of sandstone and/or siltstone. Like the sandstone, the mudstone is metamorphosed to hornfels around the granodiorite porphyry bodies.

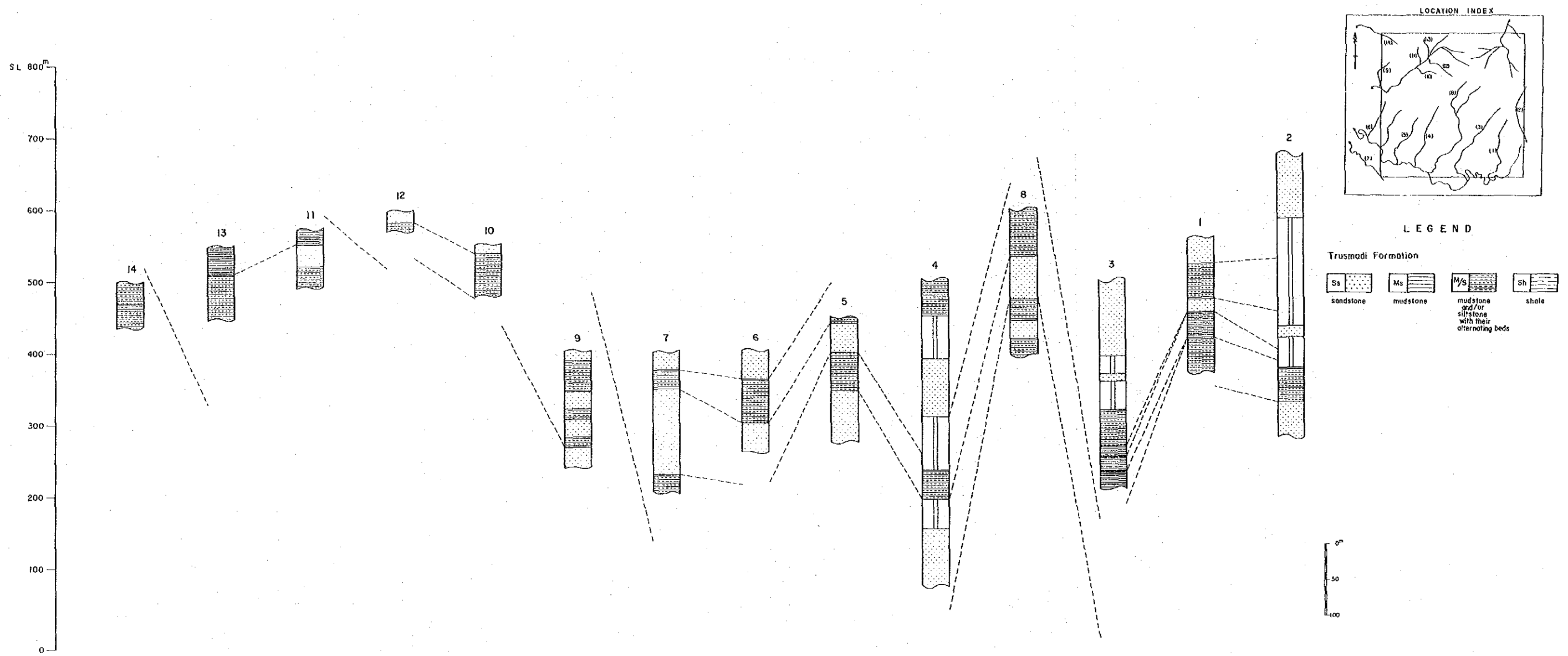


Fig. 82 Geological Columnar Sections of "c" Area

The result of microscopic study of the representative sample is as follows;

T-08 Mudstone

Grains : quartz

Characteristics : Grain size is less than 3×10^{-3} mm. No mineral other than quartz has been identified. Grading is observed; secondary sericite tends to occur along the lamina.

3) Shale facies

The remarkable character of the facies is that the color of this rock and weathered soil is red to reddish brown. It is so well bedded and well exposed laterally, that together with its color, it can be used as a key bed in the survey. The rock is fissile, rather silty, compact and hard.

1-1-2 Intrusive rock

The granodiorite porphyry is the only intrusive rock in the area.

Distribution; This intrusive body is emplaced in the northern part of the area and various sizes of stocks and dykes are intruded in the northern and central area.

Rock facies; Granodiorite porphyry which has porphyritic texture contains abundant amphibole and mica phenocrysts. The hollocrystalline groundmass has various sizes of grain locally. However, the granodiorite porphyry from various stocks and dykes have similar facies. Some of the stocks in the north-eastern and the northwestern parts of the Area show equip-granular texture. Granodiorite shows occasionally a typical onion structure.

The dykes, as small intrusives, have different mineral assemblage between the marginal and central zones. The marginal facies, is rather leucocratic and more acidic, has no colored minerals, whereas the central portions has abundant colored minerals such as amphibole, biotite and very rare pyroxene. The occurrence of this leucocratic rock facies is usually local less than several metres in width.

The result of typical specimen under the microscope is as follows;

Y-02 Granodiorite porphyry

Texture : porphyritic, hollocrystalline

Phenocrysts : plagioclase, hornblende > biotite > quartz

Characteristics : Porphyritic hollocrystalline in groundmass. The phenocrysts are mainly plagioclase, subhedral in shape with diameter of 2 mm +. A zonal structure is often observed in phenocrysts of plagioclase. Colored minerals consist of subhedral hornblende and biotite with sizes of 2 mm and 1 mm respectively. Groundmass is mainly composed of quartz and plagioclase with minor amount of biotite, hornblende and opaque minerals. Amount of altered mineral is less than that of epidote. In addition a few quartz veinlets are found with some opaque minerals.

1-1-3 Rock Composition

Four samples were chemically analysed; two were from a stock in the northeastern part of the area, one from a stock in the northwestern part, and another from a dyke in the northern central part.

Chemical analytical results and norm of these samples are shown in Table 8.

As shown in Table 8, the amount of SiO_2 is about 55 W% showing intermediate value between granodiorite and granite. The other components in each sample show very similar values. Therefore the chemical composition of the granodiorite porphyry from the stocks and dykes are similar.

The Q-Pl-Kf diagram in Fig. 83 shows that the samples plot within the area of granite, close to the boundary of granodiorite.

The intrusive rocks are identified as granodiorite porphyry according to the results of microscopic study chemical analyses.

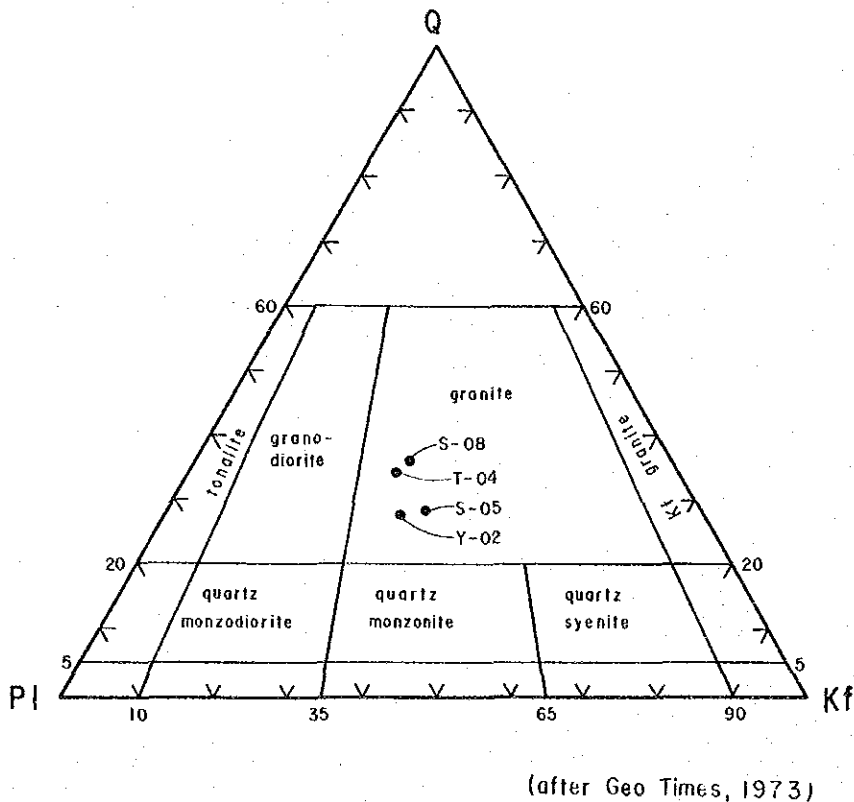


Fig. 83 Normative Q-Kf-Pl Diagram of Intrusive Rocks in "c" Area

Table 18 Chemical Composition and CIPW Norm of Intrusive Rock

Sample No.	T-04	Y-02	S-05	S-08	
Location	C36-08	C36-18	C12-09	C06-01	
Rock Name	granodiorite porphyry	granodiorite porphyry	granodiorite porphyry	granodiorite porphyry	
Chemical Composition	SiO ₂ %	66.36	66.36	65.43	65.98
	TiO ₂	0.53	0.53	0.54	0.56
	Al ₂ O ₃	12.14	13.49	12.92	13.08
	Fe ₂ O ₃	0.28	0.12	0.99	1.14
	FeO	4.92	4.69	4.24	4.05
	MnO	0.16	0.13	0.11	0.10
	MgO	3.43	2.70	3.46	2.61
	CaO	4.61	4.50	3.59	2.82
	Na ₂ O	1.74	2.25	1.82	1.68
	K ₂ O	3.62	4.19	4.58	3.92
	P ₂ O ₅	0.17	0.18	0.15	0.21
	BaO	0.57	0.60	0.65	0.86
	Ign.loss	1.66	1.29	2.03	3.99
	TOTAL	100.36	101.03	100.51	101.00

Sample No.	T-04	Y-02	S-05	S-08	
Q ^{wt%}	25.61	27.72	22.48	28.57	
c	0.00	0.00	0.00	0.88	
or	21.39	24.76	27.07	23.17	
ab	14.72	19.04	15.40	14.22	
an	14.62	14.33	13.56	14.18	
ne	0.00	0.00	0.00	0.00	
wo	0.00	0.00	0.00	0.00	
di	wo	3.41	3.30	1.86	0.00
	en	1.70	1.51	1.03	0.00
hy	fs	1.64	1.77	0.75	0.00
	en	6.84	5.22	7.58	6.50
ol	fs	6.59	6.11	5.53	5.76
	fo	0.00	0.00	0.00	0.00
	fa	0.00	0.00	0.00	0.00
mt	0.41	0.17	1.44	1.65	
ht	0.00	0.00	0.00	0.00	
il	1.01	1.01	1.03	1.06	
tn	0.00	0.00	0.00	0.00	
ru	0.00	0.00	0.00	0.00	
ap	0.39	0.42	0.35	0.49	
TOTAL	98.34	99.36	98.07	96.47	

1-1-4 Structure

There are many faulting and folding structures in the area. The N-S fault system predominates and is believed to be post Neogene. However ENE-WSW, WNW-ESE, NE-SW and NW-SE systems are also observed. Folding structures change their directions from E-W to N-S of their axes, and they are gradually converged towards southwestern part of the Area.

A structural map of the area is shown in Fig. 20.

The faulting process in this area can be assumed as follows;

N-S in central part, ENE-WSW in southeastern part, WNW-ESE, NE-SW and NW-SE in northwestern part are generally believed to have developed in this sequence. They occurred in sedimentary rock before plutonic intrusion; intrusion of the granodiorite porphyry is probably controlled by the pre-existing faults. In some places the granodiorite porphyry occur as dykes or stocks.

A N-S system in eastern part, NNE-SSW in northwestern part and NW-SE in southern part were formed during/after intrusion and/or post intrusion.

Statistical study was made using Rose diagram (Fig. 85) which shows total length and frequency at class interval of 10° of faults and direction of intrusive rock. As the result of this study, the direction of intrusion coincides nearly with the N-S direction of fault system.

The movement is rather small and local. However the N-S and NE-SW system in this area are similar to the fault structures in Kinabalu region (refer to Fig. 5).

Locally, overfolds are observed in the area and may be caused by fault movement. The overall structures in the area can be deduced as follows:

The distribution of shale as key bed shows anticlinal structure with E-W axis in the southeastern part of the area. The anticlinal structures repeat westwards but plunge to the southwest.

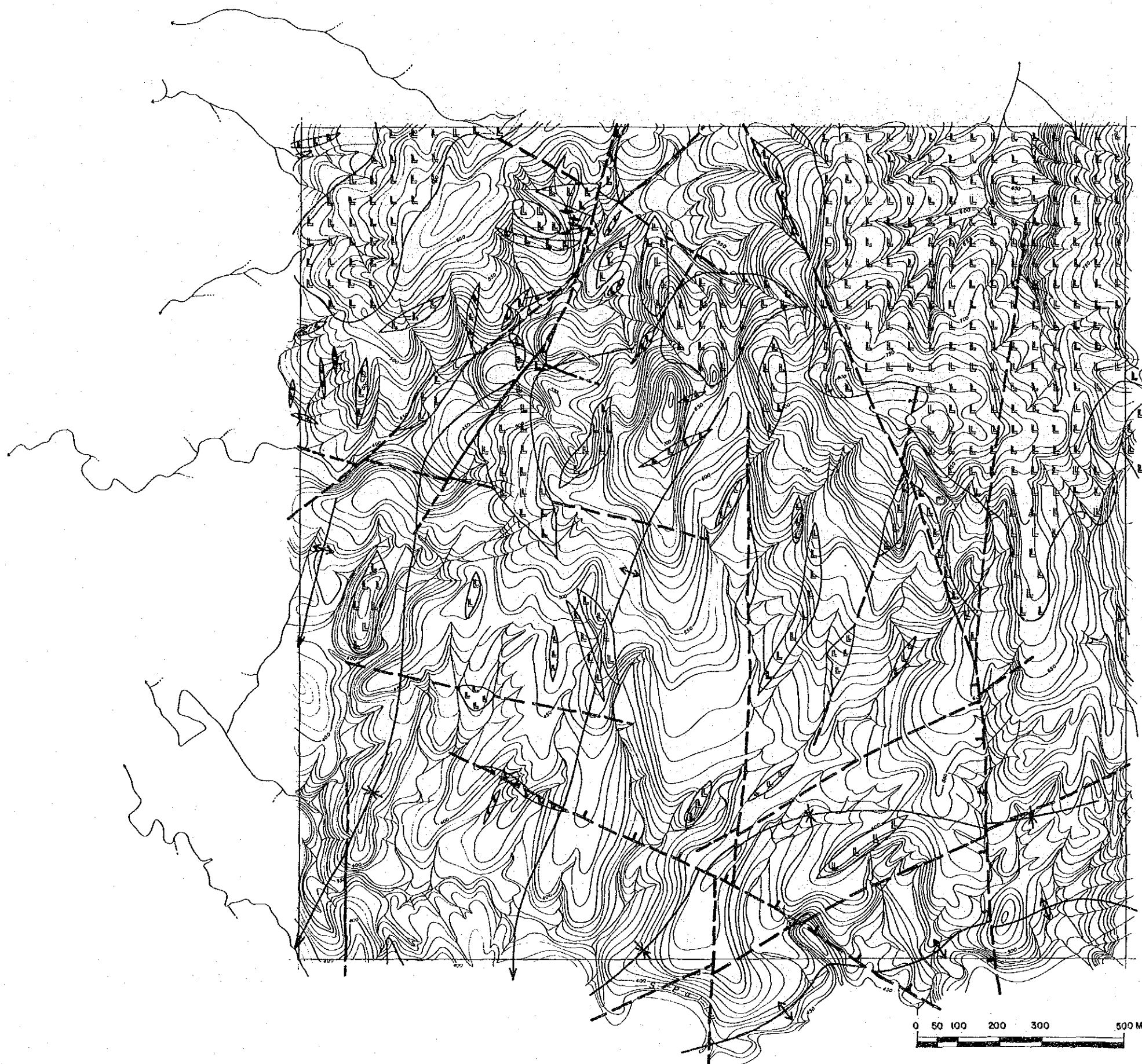
Finally the folding axis changes its direction to N-S. The inclination of strata varies from 20° to 40° in western part, 50° to 60° in southwestern part of the area.

1-2 Mineralization

It is clear that mineralization is controlled by the relationship between geological structures and plutonic intrusions, as indicated by its occurrences in vein and as dissemination. However the scale of mineralization is rather small and only a little mineral occurrence is observed.

1-2-1 Alteration

The pyrometamorphism is caused by granodiorite porphyry intrusion. Silicification and chloritization are the main alteration in the Area. The sedimentary rock in the Area were altered to hornfels by pyrometamorphism of intrusive bodies, especially in the northern part of the Area.



LEGEND


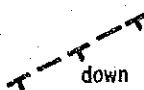
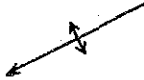

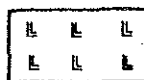
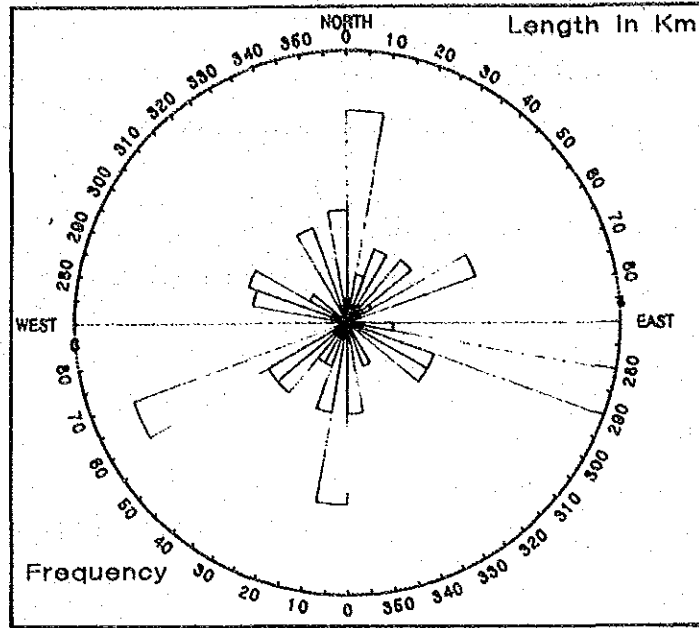
-  fault (certain)
-  fault (inferred)
-  anticline with plunge direction
-  syncline with plunge direction
-  granodiorite porphyry

Fig. 84 Structural Map of "c" Area

(Faults)



(Intrusive Rock)

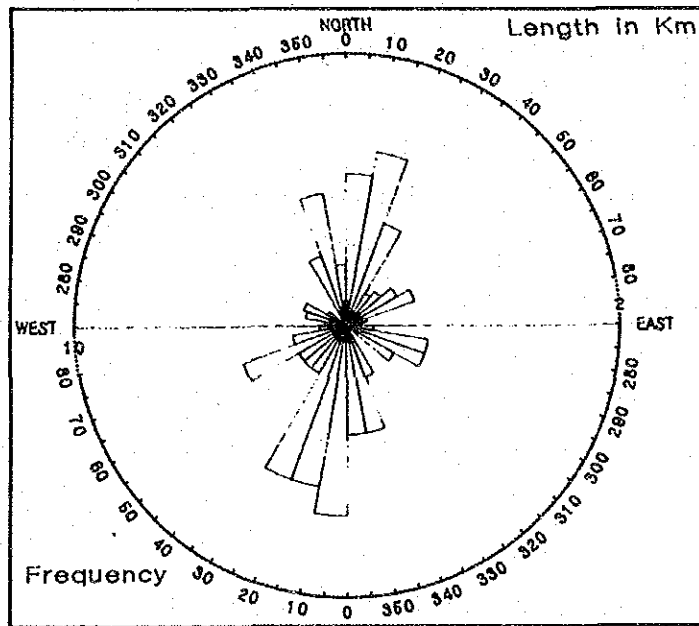


Fig. 85 Rose Diagram of Structural Elements in "c" Area

Near intrusive bodies silicification with irregular shape quartz veinlets occurred in the sedimentary rocks (Fig. 86). This silicification is widespread in the southern and southwestern parts of the intrusive stock, and is scattered over the area surrounding the small intrusive bodies in the western half. Generally speaking the silicification is stronger in the eastern part than the western part.

Weak chloritization is also found in intrusive stocks and dykes.

The pelitic rock has sericite-chlorite (-epidote) alteration as regional metamorphism. Calcite is also common in the area.

1-2-2 Mineralization

Vein-type and disseminated mineralization are related to the intrusion of granodiorite porphyry is found in the (1) eastern to central part of the area and (2) northwestern to western part (refer to Fig. 86).

(1) Eastern to central part

Mineralization is found in sedimentary rock in the southern and southwestern periphery of granodiorite porphyry stock. They occur as stringers and/or disseminated pyrite mineralization with quartz veinlets (less than few centimetres in width). Locally the southern part of this mineralized zone is characterized by bleaching, with pyrite and a very small amount of chalcopyrite. This mineralized zone may extend eastward.

In the central area the silicification, affected by intrusives, is strong and a number of quartz veinlets is also found. The veins consist of some sulfide minerals. However most of them are barren. One vein reached 1 m in width and is surrounded by veinlets of less than 5 cm. Silicification of the sedimentary rocks have made them resistant to weathering, forming steep cliffs.

The sketch for the above mentioned quartz vein which was found in the central part of this area is shown in Fig. 23. The quartz vein occurs in rhythmical alternating beds of sandstone and mudstone. It seems to be a stock-shaped infilling in sedimentary rock, not as infilling in structural fissure. It contains abundant arsenopyrite with minor pyrite. Microscopic study of the representative samples are as follows;

Y-20 (1) Arsenopyrite ore

Ore minerals : arsenopyrite \gg pyrite \gg chalcopyrite, covellite

Characteristics : Predominantly arsenopyrite, coarse to fine grained and light cream or pinkish white in color; it is distinguished from pyrite by its anisotropy. The crystals have sharp boundaries with irregular sparse or dense fine cracks. Many fine pyrite crystals are observed in the area of 0.7 mm x 0.6 mm, with a small amount of chalcopyrite. The chalcopyrite and covel-

lite are found in the interspaces between arsenopyrite crystals and are formed in a later stage.

Lead and zinc minerals are not detected.

The result of chemical analysis for same sample is as follows;

	Au(g/t)	Cu(%)	Pb(%)	Zn(%)	Mo(%)	Hg(%)	As(%)	S(%)
Y-20(1)	1.40	0.13	0.02	0.02	0.001	0.001	41.82	17.67
Y-20(2)	2.13	0.02	0.02	0.02	0.001	0.001	—	—

Granodiorite porphyry has little mineralization.

(2) Northwestern and western part

The mineralization in the area is also related to granodiorite porphyry intrusion. The size of intrusive bodies varies from 10 m to several 100 m in diameter. The mineralization, disseminated and vein-type, is mainly confined to sedimentary rocks at the boundary of intrusive bodies. The mineral assemblage of the intrusives in the marginal zone is different. In this zone pyrite and minor amount of chalcopyrite have been recognized. The width of mineralization is only few metres from contact of both rocks (Fig. 24). Pyrrhotite and pyrite have been identified.

The results of microscopic observation of three representative samples are as follows;

S-20 Pyrrhotite — quartz veinlet

Ore minerals : pyrrhotite \gg pyrite, sphalerite, galena

Characteristics : Sulfide-quartz veinlet in mud-stone facies. Sulfide minerals are mainly pyrrhotite with very small amount of pyrite, sphalerite and galena. Pyrrhotite is dispersed in veinlets and are subhedral to anhedral in shape.

Amount of pyrite is rather small compared to pyrrhotite, and it is accompanied with pyrrhotite in the host rock. Ratio of sphalerite to pyrite is about 1 and it occurs as inclusions of fine crystals of 0.3 mm, in the pyrrhotite. Chalcopyrite is finer and of less amount.

Y-14 Sulfide impregnated granodiorite porphyry

Ore minerals : pyrite, pyrrhotite $>$ chalcopyrite, sphalerite, galena

Characteristics : The intrusive has been impregnated by minor amount of sulfide. No quartz veinlet is found. A clear porphyritic texture has been observed. Ore minerals show irregular and anhedral shaped and very fine grained, filling the spaces of host rock minerals.

Y-12 Veinlet bearing granodiorite porphyry

Ore minerals : pyrite, sphalerite, magnetite, ilmenite, molybdenite

Characteristics : This specimen has been collected from the marginal part of the intrusives. The mineralization itself is weak, with few-veinlets. Primary fine magnetite and ilmenite are dis-



LEGEND



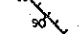
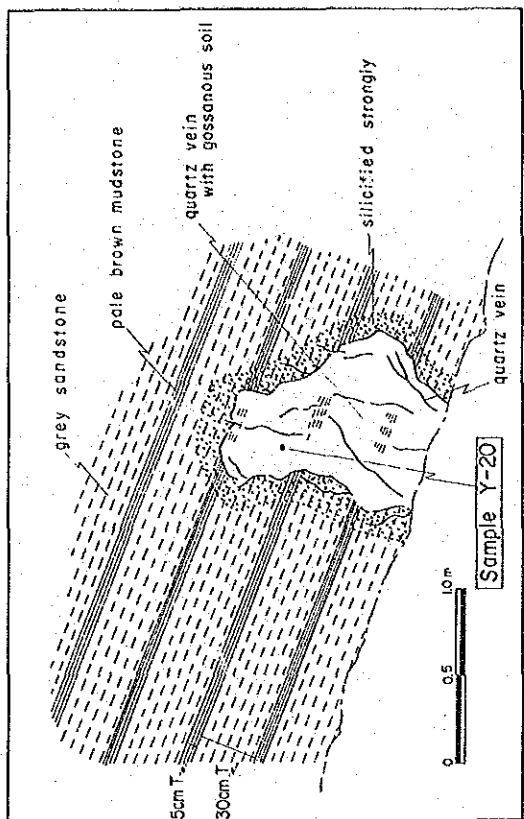
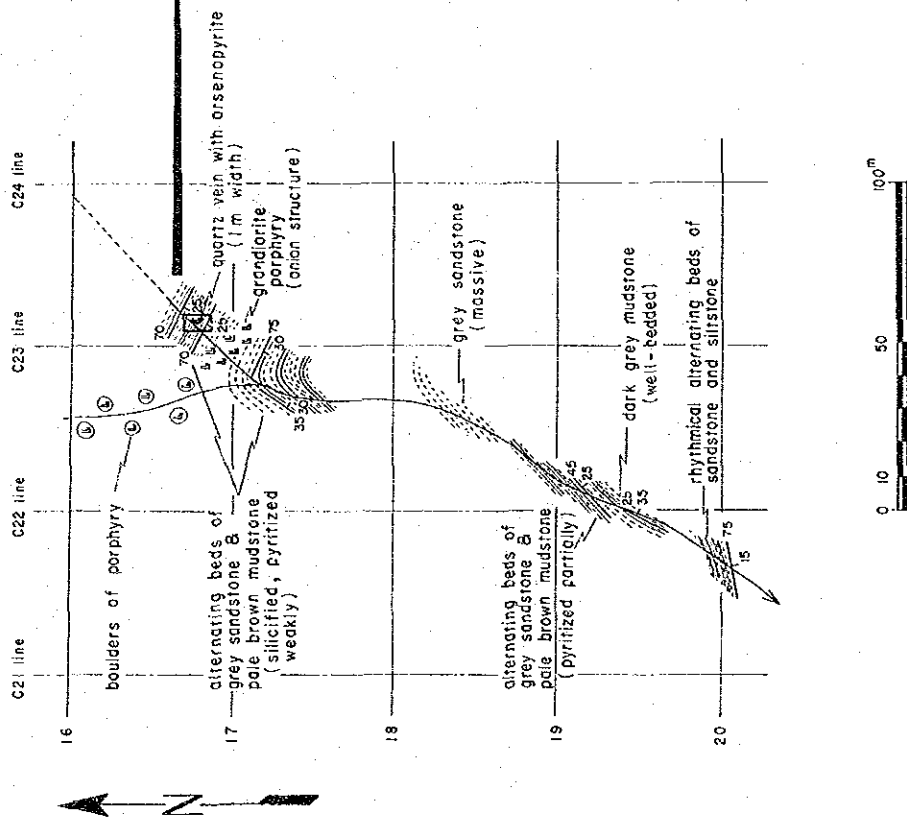
-  silicification
-  pyritization
-  quartz vein

Fig. 86
Distribution of Alteration Zone in "c" Area



Sample Y-20
 arsenopyrite ore
 vein type, arsenopyrite, massive, arsenopyrite, euhedral to subhedral, especially euhedral crystals of quartz and arsenopyrite in druses (5 cm big), with white colored amorphous silica
 boundaries : irregular, not clear

Fig. 87 Sketch Showing Quartz Vein

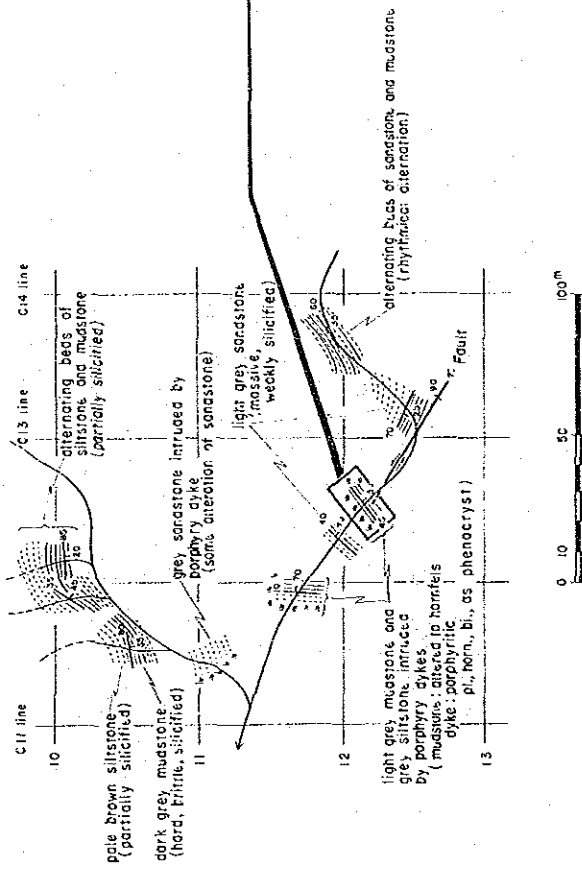
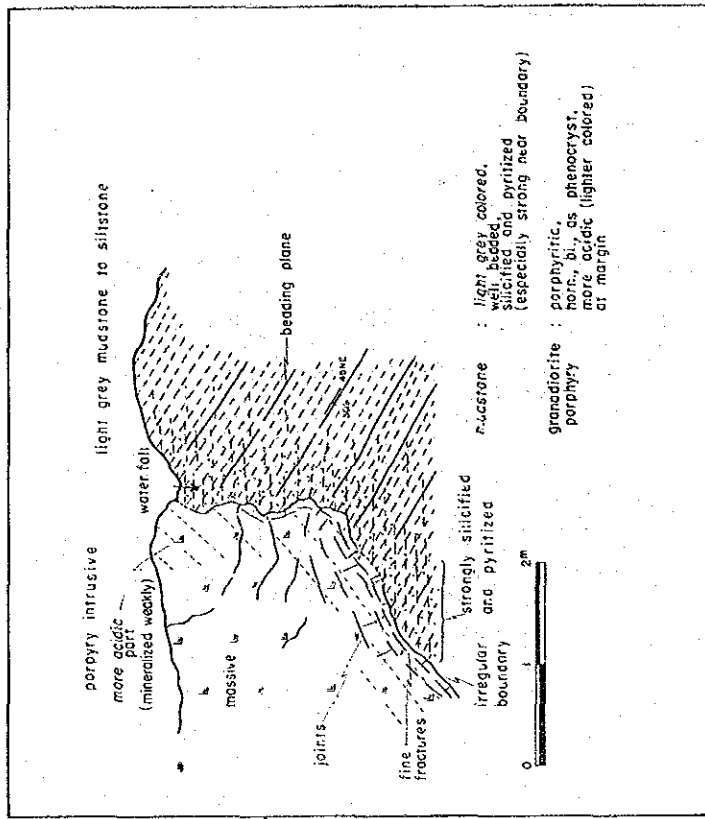


Fig. 88 Sketch Showing Mineralization by Intrusive Rock

persed within the host rock. Uncertain molybdenite has been detected. Streak has fine grained pyrite with minor amount of sphalerite, and no gangue mineral has been observed.

The mineralization in the area described above is considered to be weak and is related to intrusion of granodiorite porphyry. From this point of view, distribution of mineralized zones shall be limited to the marginal parts of intrusive bodies.

Chapter 2 Geochemical Survey

2-1 Soil Survey

2-1-1 Field Procedure and Data Analysis

Soil samples were collected for chemical analysis in a grid system of 50 x 50 meters as well as those in the "b" area.

A histogram and a cumulative frequency curve for each rock facies were produced based on the analytical data (Figs. 90, 91).

A value of $\bar{X} + 2t$, occupying 2.5 per cent of the entire population, was taken as the threshold value. Using this value, geochemical anomaly map was made with supplementary values of $\bar{X} + t$ and $\bar{X} + 3t$.

The statistic values for each element and each rock facies are shown in Table 19.

2-1-2 Result of Survey

The distribution of each of the four elements such as Cu, Pb, Zn and Au among the five elements chemically analyzed was plotted on the 1 : 5,000 scale topographical maps. Regarding Au, 1,148 assay values of the samples collected from the survey lines from No.1 to No.28 were provided for analysis. On the other hand, the assay results of Mo were used only for reference because 97.3 per cent of the whole samples were below the detection limit.

These elements were evaluated by score sum as in the procedure of analysis for the "b" area, and factor analysis was also used. The results were comprehensively evaluated. The results were indicated on the 1 : 5,000 scale topographical map.

(1) Distribution of Elements

(i) Copper (Cu)

The maximum assay value was shown to be 462 ppm and the minimum 1 ppm, varying greatly in distribution of the assay values for each rock facies. When the mean values are reviewed for example, 41.3 ppm is obtained in the intrusive rocks and 14.3 ppm in the sedimentary rocks, showing a low value in the latter. From this, it is considered to be very significant also in this area to classify the rock facies (Map 64).

The classification of the rocks into the intrusive rocks and the sedimentary rocks led to be able to extract the main part of the values larger than $\bar{X} + 2t$.

They are distributed mainly in the terratin of sedimentary rocks in the neighborhood of the contact with the intrusive rock. Especially, they are concentrated around the stock found in the northeastern part of the survey area. A few of them are found in the stock. The others are

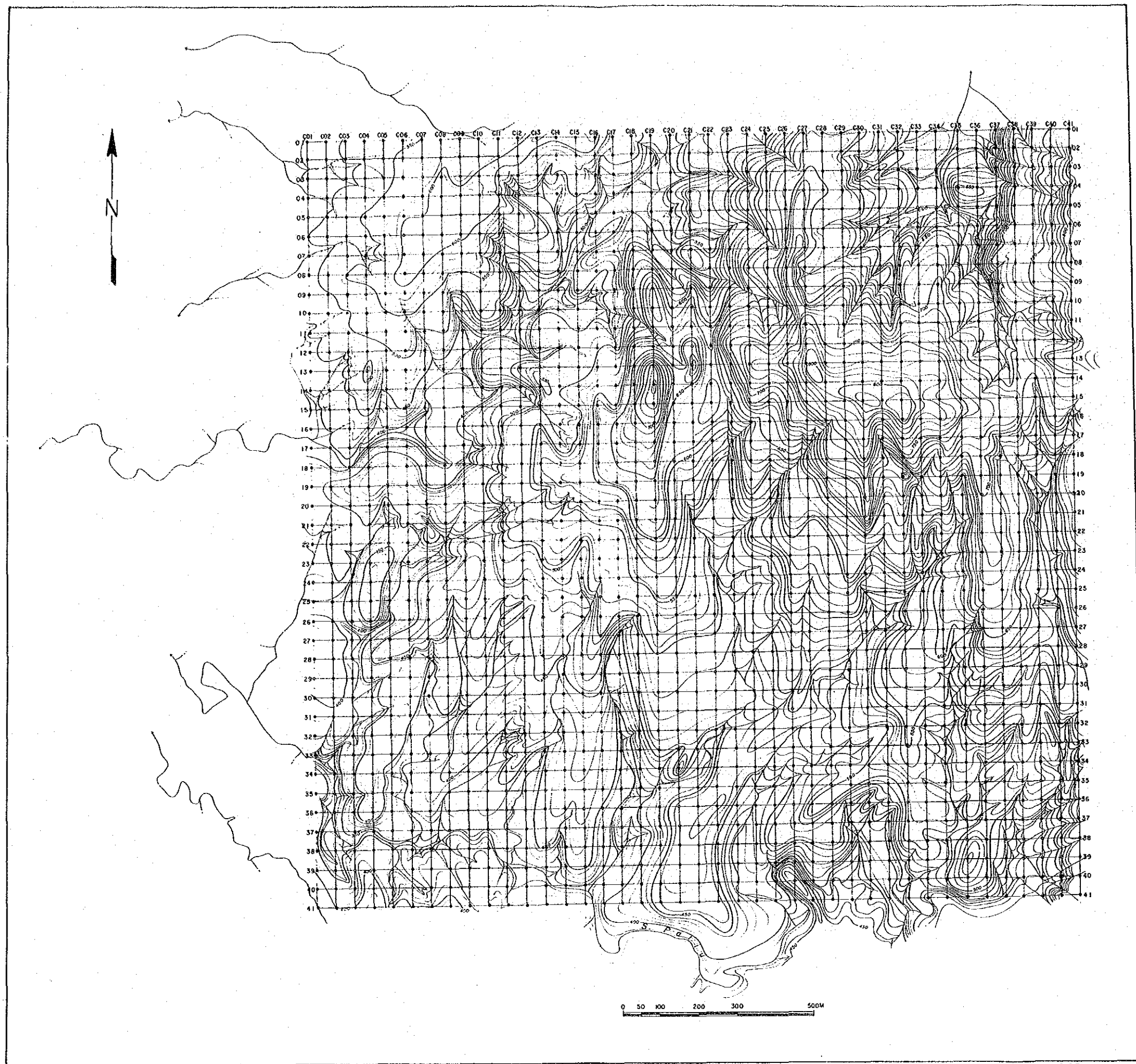


Fig. 89

Location Map of Soil Samples in "c" Area

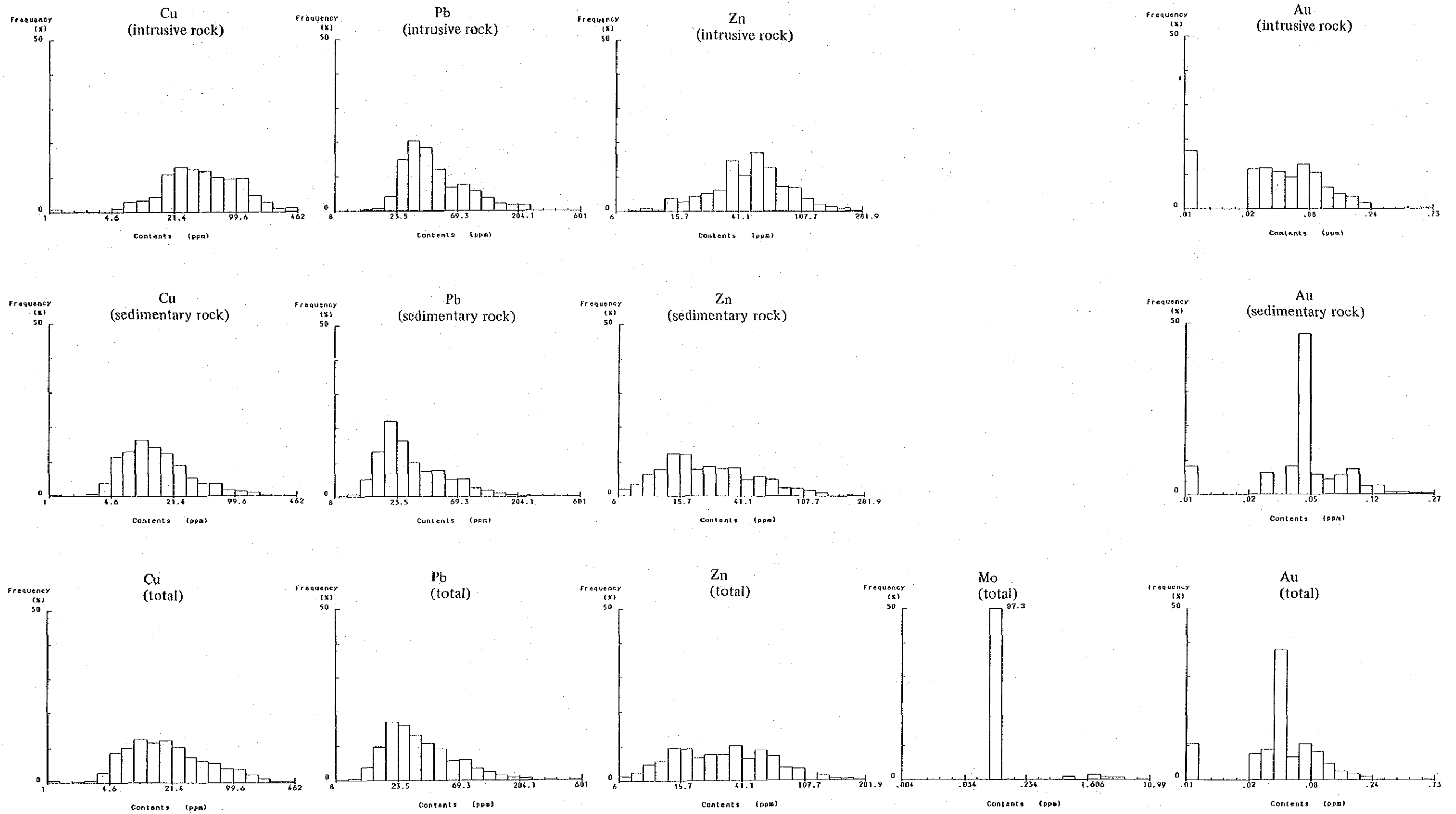


Fig. 90 Histogram for Soil Samples in "c" Area

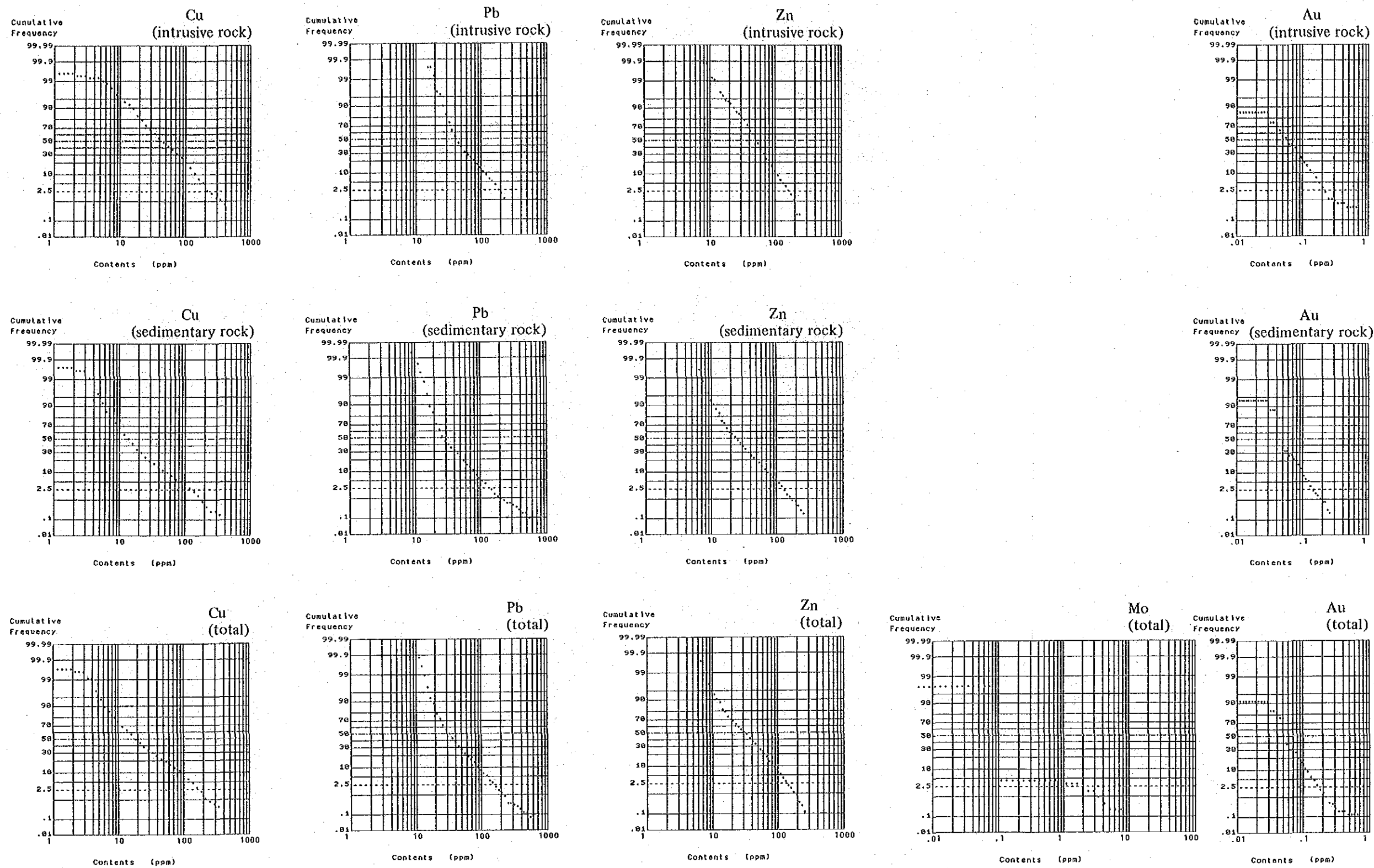


Fig. 91 Cumulative Frequency Curve for Soil Samples in "c" Area

Table 19 Statistic Values for Soil Samples in "c" Area

			Intrusive rock	Sedimentary rock	Total
Cu (ppm)	Number of samples (n)		480	1201	1681
	Maximum value (Vmax)		462	383	462
	Minimum value (Vmin)		1	1	1
	Geometric mean (\bar{X})		41.3	14.3	19.4
	Standard deviation (t)		0.409	0.379	0.440
	$10^{\log\bar{x}+t}$		105.9	34.2	53.4
	$10^{\log\bar{x}+2t}$		271.6	81.9	147.2
	$10^{\log\bar{x}+3t}$		(695.5)	196.0	405.3
Pb (ppm)	Number of samples (n)		480	1201	1681
	Maximum value (Vmax)		235	601	601
	Minimum value (Vmin)		14	8	8
	Geometric mean (\bar{X})		46.1	31.0	34.7
	Standard deviation (t)		0.244	0.266	0.271
	$10^{\log\bar{x}+t}$		80.9	57.2	64.8
	$10^{\log\bar{x}+2t}$		141.8	105.5	120.9
	$10^{\log\bar{x}+3t}$		(248.7)	194.7	225.6
Zn (ppm)	Number of samples (n)		480	1201	1681
	Maximum value (Vmax)		250	282	282
	Minimum value (Vmin)		8	6	6
	Geometric mean (\bar{X})		48.1	24.4	29.7
	Standard deviation (t)		0.262	0.323	0.335
	$10^{\log\bar{x}+t}$		87.9	51.3	64.2
	$10^{\log\bar{x}+2t}$		160.7	108.0	138.9
	$10^{\log\bar{x}+3t}$		(293.9)	(227.2)	(300.4)
Mo (ppm)	Number of samples (n)		480	1201	1681
	Maximum value (Vmax)		11	5	11
	Minimum value (Vmin)		ND	ND	ND
	Geometric mean (\bar{X})		-	-	-
	Standard deviation (t)		-	-	-
	$10^{\log\bar{x}+t}$		-	-	-
	$10^{\log\bar{x}+2t}$		-	-	-
	$10^{\log\bar{x}+3t}$		-	-	-
Au (ppm)	Number of samples (n)		470	680	1150
	Maximum value (Vmax)		0.72	0.23	0.72
	Minimum value (Vmin)		ND	ND	ND
	Geometric mean (\bar{X})		0.049	0.048	0.048
	Standard deviation (t)		0.337	0.314	0.352
	$10^{\log\bar{x}+t}$		0.106	0.099	0.108
	$10^{\log\bar{x}+2t}$		0.231	0.204	0.243
	$10^{\log\bar{x}+3t}$		0.503	(0.420)	0.546

note) () ; value not present

Correlation Matrix

	Intrusive rock			Sedimentary rock			Total		
	Cu	Pb	Zn	Cu	Pb	Zn	Cu	Pb	Zn
Pb	-0.030	-	-	0.494	-	-	0.298	-	-
Zn	0.363	0.603	-	0.589	0.755	-	0.546	0.698	-
Au	0.199	0.004	-0.023	0.174	0.052	0.009	0.174	0.032	-0.002

mostly detected in the vicinity of the dykes distributed in the central part of the survey area.

(ii) Lead (Pb)

The distribution of Pb is indicated on Map 65. The assay values range from the maximum of 601 ppm to the minimum of 8 ppm.

The mean values for each rock facies are 46.1 ppm in the intrusive rock and 31.0 ppm in the sedimentary rock.

The samples showing the values larger than $\bar{X} + 2t$ are generally distributed in the north-central part of the survey area.

But the distribution is slightly different from that of the values larger than $\bar{X} + 2t$ of Cu. In the case of Cu, the zones are generally distributed on the south of the stock in the north-eastern part of the survey area, but in the case of Pb, they are rather distributed on the west of it. They are also found in the vicinity of small stocks and dykes in the north-central part of the survey area.

(iii) Zinc (Zn)

The distribution of zinc is indicated on Map 66.

The assay values range from the maximum of 282 ppm to the minimum of 6 ppm. The mean values are 48.1 ppm in the intrusive rock and 24.4 ppm in the sedimentary rock. The former is about twice the latter.

The distribution of values larger than $\bar{X} + 2t$ is generally consistent with that of Pb, which leads to an assumption that the correlation between Pb and Zn is high. Therefore, the distribution of the samples showing the values larger than $\bar{X} + 2t$ appear on the west of the stock in the northeastern part of the survey area and in the neighborhood of the stocks or dykes found from the center to the north-center part.

(iv) Molybdenum (Mo)

The distribution of molybdenum is indicated on Map 67.

The assay values range from the maximum of 11 ppm to the value below the detection limit. Those below the detection limit occupy 77.3 per cent of the whole samples.

The distribution of the samples showing the values above the detection limit is not consistent with those of Cu, Pb and Zn in general, but has a tendency to be found in the surrounding area of the values larger than $\bar{X} + 2t$ of these elements.

(v) Gold (Au)

A distribution of Au is indicated on Map 68. Samples of 1,150 PCS were analyzed for gold.

The assay values range from the maximum of 0.72 ppm to the value below the detection limit (= 0.3 ppm). The distribution of Au is different from the other four elements, showing

very low correlation with them.

The zones distributed by the values larger than $\bar{X} + 2t$.

The distribution of values larger than $\bar{X} + 2t$ generally tends to be scattered inside the area distributed by the intrusive rocks, especially a wide distribution is shown in the stock located in the northeastern part of the survey area.

(2) Result of Score Sum Analysis

The result of analysis by score sum is shown on Map 23.

The elements utilized for the map were those such as Cu, Pb, Zn and Au. Mo was excluded from the map by the reason that it was difficult to give adequate score because 97.3 per cent of the whole assay values were below the detection limit.

Because the total number of Au analysis was 1,150 as mentioned before, the scores were given utilizing the assay results of No. 1 to No. 28 of each survey line. As a result, the number of elements used for the score sum map was different between the northern part of the survey area (from No.1 to No.28 of each survey line) and the southern part (from No.29 to No.41 of each survey line), such as four elements in the northern part and three elements in the southern part respectively. However, no notable indication is not shown in reference to Cu, Pb and Zn in the southern part. Therefore, the result of analysis will be described for the northern part of the survey area (No.1 to No.28 of each survey line).

The highest score obtained in the area was nine, and they were located in the vicinity of C15-21 and C22-13. The distribution of the score (6-7) following the above was found in the vicinity of C15-21 and in the western part and the southwestern part of granodiorite located in the northeastern part of the Area. The score lower than the aboves are found in the surrounding area of the zones mentioned before, in the surrounding area of the dykes in the northwestern part of the area and in a part of the area where granodiorite porphyry stock is exposed in the northeastern part.

The following facts can be recognized from the distribution in the above.

(i) The score sum map shows a very good consistency with the geologic map, and the high-score area is limited to the stock of granodiorite porphyry or in the sedimentary rocks around the dykes.

(ii) In the sedimentary rocks in the surrounding area of the granodiorite mass located in the northeastern part of the survey area, the high-score zones are distributed in such a way to surround the mass, especially in the southwestern side.

(iii) No mineralization is observed in the vicinity of granodiorite stocks and dykes distributed in the western part of the survey area.

(iv) The area which seems to be most promising is found in the vicinity of C15-21, showing an extent of about 15,000 square meters on the surface.

(3) Result of Factor Analysis

The samples (1,148 pcs in total) of No.1 to No.28 of each survey line were analyzed for four elements, such as Cu, Pb, Zn and Au. Interpretation was made for two cases such as the one in which the assay values were treated without classification of rock facies and the other in which the rocks were classified into granodiorite porphyry and the sedimentary rocks. Factor loading, factor contribution and communality of each factor are shown in Table 20. The distribution of factor scores is shown on Map 70-72.

The characteristic of each factor is as follows.

Unclassified Rock Facies:

Factor-1 is a factor related to Pb-Zn. The factor loading is showing high values of 83.2 for Pb and 69.6 for Zn. The factor contribution is 55.1 per cent, and the variation explained by this factor is more than half. The communality of Pb and Zn are 0.720 and 0.752 respectively, showing a good explanation for the variation of these elements.

Factor-2 is the one related to Cu-Zn, and the factor loading is 67.1 per cent for Cu and 51.7 per cent for Zn. The factor contribution is 33.7 per cent, showing that the variation explained by Factor-1 and Factor-2 reaches 89.2 per cent.

Factor-3 is the one related to Au (-Cu). The respective factor loading is low and the factor contribution is as low as 10.8 per cent. The low communality of Au of 0.187 easily leads to the assumption that the distribution of Au is different from those of other three elements.

Classified Rock Facies:

(a) Terrain of Granodiorite

Factor-1 is the one related to Pb-Zn. The factor loading is 80.4 per cent for Pb and 70 per cent for Zn respectively, showing high values of loading. The factor contribution is 58.1 per cent, occupying more than half. The communality of Pb and Zn are 0.649 and 0.678 respectively, showing a good explanation for the variation of these elements.

Factor-2 is the one related to Cu-Zn, and the factor loading is as high as 60.8 per cent for Cu and 43.2 per cent for Zn respectively. The factor contribution is 29.1 per cent. Thus 87.2 per cent of the whole samples could be explained by Factor-1 and Factor-2.

Factor-3 is the one related to Au (-Cu). The communality is as low as 0.218, and it seems that Au shows a behavior different from other elements.

Table 20 Result of Factor Analysis

Total factor loadings

	factor-1	factor-2	factor-3
Cu	0.246	0.671	0.243
Pb	0.832	0.167	0.017
Zn	0.696	0.517	-0.032
Au	-0.006	0.081	0.424

factor contribution

factor	contribution	%	acc.%
1	1.236	55.5	55.5
2	0.752	33.7	89.2
3	0.240	10.8	100.0

Communarity

Cu	Pb	Zn	Au
0.570	0.720	0.752	0.187

Intrusive Rock factor loadings

	factor-1	factor-2	factor-3
Cu	0.065	0.608	0.216
Pb	0.804	-0.047	-0.010
Zn	0.700	0.432	-0.047
Au	-0.020	0.116	0.452

factor-contributions

factor	contribution	%	acc. %
1	1.142	58.1	58.1
2	0.571	29.1	87.2
3	0.253	12.9	100.1

Communarity

Cu	Pb	Zn	Au
0.420	0.649	0.678	0.218

(continued)

Sedimentary Rock factor loadings

	factor-1	factor-2	factor-3
Cu	0.482	0.521	0.308
Pb	0.862	0.132	0.062
Zn	0.804	0.366	-0.015
Au	0.011	0.156	0.423

factor contribution

factor	contribution	(%)	acc.950
1	1.621	69.7	69.7
2	0.426	18.3	88.0
3	0.278	12.0	100.0

Communarity

Cu	Pb	Zn	An
0.598	0.764	0.780	0.182

(b) Terrain of Sedimentary Rock

The same can be said in the case of sedimentary rock as in that of granodiorite.

Factor-1 is related to Pb-Zn and Factor-2 to Cu-Zn. By these two factors, 88 per cent of the whole samples can be explained. Factor-3 is the one related to Au (-Cu).

Distribution of Factors will be discussed.

Unclassified Rock Facies:

Factor-1 (Pb-Zn) is widely distributed from the western part to the central part of the granodiorite mass which is located in the northeastern part, and also found in the area distributed by the swarm of small dykes in the northwestern part of the area and in the vicinity of C15-21.

Factor-2, on the other hand, is distributed from the southern part to the southwestern part of the granodiorite stock in the northeastern part of the area.

Thus Factor-1 and Factor-2 are distributed in two areas separated considerably.

The areas distributed by Factor-1 are mainly consistent with the silicification zone or weakly silicified zone spread over the surrounding area of the stocks or dyke swarms, and it is assumed that the mineralization is characterized by the factors explained by combination of Pb-Zn. However, a part of it extends into the inside of intrusive granodiorite.

Factor-2 is mainly distributed in the stock found in the northeastern part of the area, and characterized by the combined factors of Cu-Zn. Factor-2 has a strong tendency to be controlled by rock facies, and the effect of rock facies may be a main cause of this factor.

Classified Rock Facies:

(a) Granodiorite (Map 71)

Factor-1 (Pb-Zn) is scatteringly distributed in a part of the stock in the northeastern part of the area, in a small stock in the central-northern part, in a small dyke swarm to the northeast of it and in small dykes in the central part.

Factor-2 (Cu-Zn) tends to be scattered mainly in the stock located in the northeastern part of the area. It leads to the recognition that they are possible to be classified even in the same granodiorite by each factor by respective combination of Pb-Zn and Cu-Zn. Especially, in the stock located in the northeastern part of the Area, it is shown that this tendency varies with the zones.

(b) Sedimentary Rock (Map 72)

In the case of the sedimentary rock, Factor-1 (Pb-Zn) is distributed on the southwestern side and the southeastern side of the stock in the northeast part of the area, and also in the vicinity of C15-21.

Factor-2 (Cu-Zn) has a tendency to be distributed in a belt surrounding the area distributed by Factor-1 mentioned above. This leads to an assumption of possibility that Factor-1 and Factor-2 show the zonal distribution toward the outside centering on the intrusive body.

Further consideration on the distribution shown on Map 71 lead to the recognition that the zonal distribution is characterized by the factors by combination of Pb-Zn and Cu-Zn in such a way that Pb-Zn is distributed directly inside and outside of the boundary between granodiorite and the sedimentary rock, and that Cu-Zn forms the zone toward the outside of the above.

Furthermore, when Map 70 is compared with Map 72, it is clear that the sedimentary terrain adjacent to the western end of the stock in the northeastern part of the area is explained by the different factors of each Factor-1 (Pb-Zn) and Factor-2 (Cu-Zn). It is judged that this is resulted from that the assay value of Zn depends upon the both factors and that it is influenced by classification of the rock facies.

2-1-3 Discussion

The analysis was made by the procedures such as single component, score sum and factor analysis for the geochemical survey data of the area. Fig. 32 (Map 27) show the result of analysis together with that of geologic mapping.

From the analysis diagram, (1) the area centering on C15-21 and (2) the terrain of sedimentary rock adjacent to the stock in the northeastern part of the area, especially the southwestern part of the stock, were extracted as the geochemical anomalous zones.

The distribution of these zones is well consistent with the result of geologic mapping, and silicification and/or weak mineralization are observed there.

The supplementary use of the above analysis was effective to elucidate the mineralization of the area. The details are as follows.

(1) The analysis by score sum was able to treat all the elements analysed collectively for the extraction of geochemical anomalous zone, and it was effective in the point to rank the potential of the zones.

(2) Factor analysis was important to know the behavior of each element in more detail for the geochemical anomalous zones in the above. Especially, a zonal distribution was recognized by the factors which characterize Pb-Zn and Cu-Zn.

(3) The classification of rock facies was important for obtaining the result of analysis as proved by simple element analysis. That is, it is necessary to analyze separately for each rock facies because of its different background value.



LEGEND


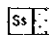

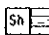
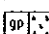

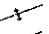
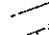
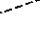
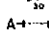



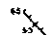
-  anomalous zone
- Trusmodi Formation**
 -  sandstone
 -  mudstone
 -  shale
- Intrusive Rock**
 -  granodiorite porphyry
-  Syncline
-  Anticline
-  Fault (certain)
-  Fault (inferred)
-  Strike and dip
-  Geological Profile line
-  silicification
-  pyritization
-  quartz vein



Fig. 92
Geochemical Interpretation Map of "c" Area

2-2 Drainage Survey

2-2-1 Field Procedure

Silty stream sediment under 80 mesh deposited at the bottom of stream was collected for the geochemical samples.

The samples were collected in the middle of the stream as principle, and consideration was given not to be contaminated by mud and organic matter. The samples were taken at an interval of 50 meters as shown in Fig. 93 (Map 74). Samples of 665 pcs were collected by these methods, which were dried in natural atmosphere and provided for chemical analysis.

2-2-2 Laboratory Procedure

The samples prepared at the site were all sent to the Geological Survey of Malaysia, Sabah, where they were analyzed by atomic absorption method in the same way as the soil samples. The samples were analyzed for four elements such as Cu, Pb, Zn and Mo.

The detection limit was 1 ppm for each element.

2-2-3 Data Analysis

For treatment of the data, simple statistical analysis and multivariate analysis were performed as in the case of soil. Therefore, it is desirable to refer to Section 2-3 of Chapter 2 in Part III for the detail. The difference is as follows.

As the effect of classification of rock facies was not so clear in simple statistical analysis, the analytical values of all the samples were treated in the lump together. Histogram and cumulative frequency curves are as shown in Fig. 94 and Fig. 95. Table 21 shows the statistical values and correlation coefficient.

In multivariate analysis, only score sum method was used for examination. As 99 per cent of Mo assay values were below detection limit among the four elements analyzed, Mo was not able to be processed.

2-2-4 Result of Survey

(1) Distribution of Elements

(i) Copper (Cu)

Map 75 shows the distribution of Cu.

The assay values range from the maximum of 58 ppm to the minimum of 1 ppm, and the mean is 19.4 ppm. It is evident that the mean value is about half that of soil sample.

The assay values larger than $\bar{X} + 2t$ is distributed as follows.

In the intrusive rock in the northeastern part of the area (in the vicinity of sample No.461 to 469).

In the surrounding area of the intrusive rock in the northeastern part of the area (sample Nos. 82, 146, 355, 356 and 367).

In the middle reaches of a northeasterly trending creek in the northwestern part of the Area (sample Nos.53 and 55).

In the upper reaches of a north-northeasterly trending creek in the southwestern part of the Area (sample Nos.578 and 582)

The locations of these tends to be distributed mainly in the upstream of the tributary creeks in the central part to the northeastern part of the survey area. The values are generally low in the southern part and the western part.

(ii) Lead (Pb)

The distribution of Pb is indicated on Map 76.

The maximum assay value is 90 ppm and the minimum 4 ppm, and the mean is 17.6 ppm, showing about half that of the soil samples same as in the case of Cu.

The values larger than $\bar{X} + 2t$ are distributed as follows.

In the intrusive rock in the northeastern part of the area (sample Nos.42 to 46).

In the tributary of a northeasterly trending creek in the northwestern part of the area (sample Nos.62 to 66, 73 to 75, 79, 93 and 94).

In the upper reaches of a northerly trending creek in the central part of the area (sample Nos.376 and 386 to 389).

In the uppermost reaches of a north-northeasterly trending branch creek in the southwest-ern part of the area (sample No.582).

Among these, Nos.68 and 389 shows the value larger than $\bar{X} + 3t$, Pb generally tends to be distributed in the different areas distributed by Cu.

(iii) Zinc (Zn)

The distribution of Zn is indicated on Map 77.

The maximum and the minimum assay values are 154 ppm and 5 ppm respectively, and the mean is 24.0 ppm, which is almost the same as that in the case of soil samples.

The values larger than $\bar{X} + 2t$ are distributed as follows.

In the intrusive rock in the northeastern part of the area (sample No.42 to 46).

In the middle reaches of a northeasterly trending creek and the branch of it in the north-western part of the Area (sample Nos.47, 66, 68, 70, 82 and 93).

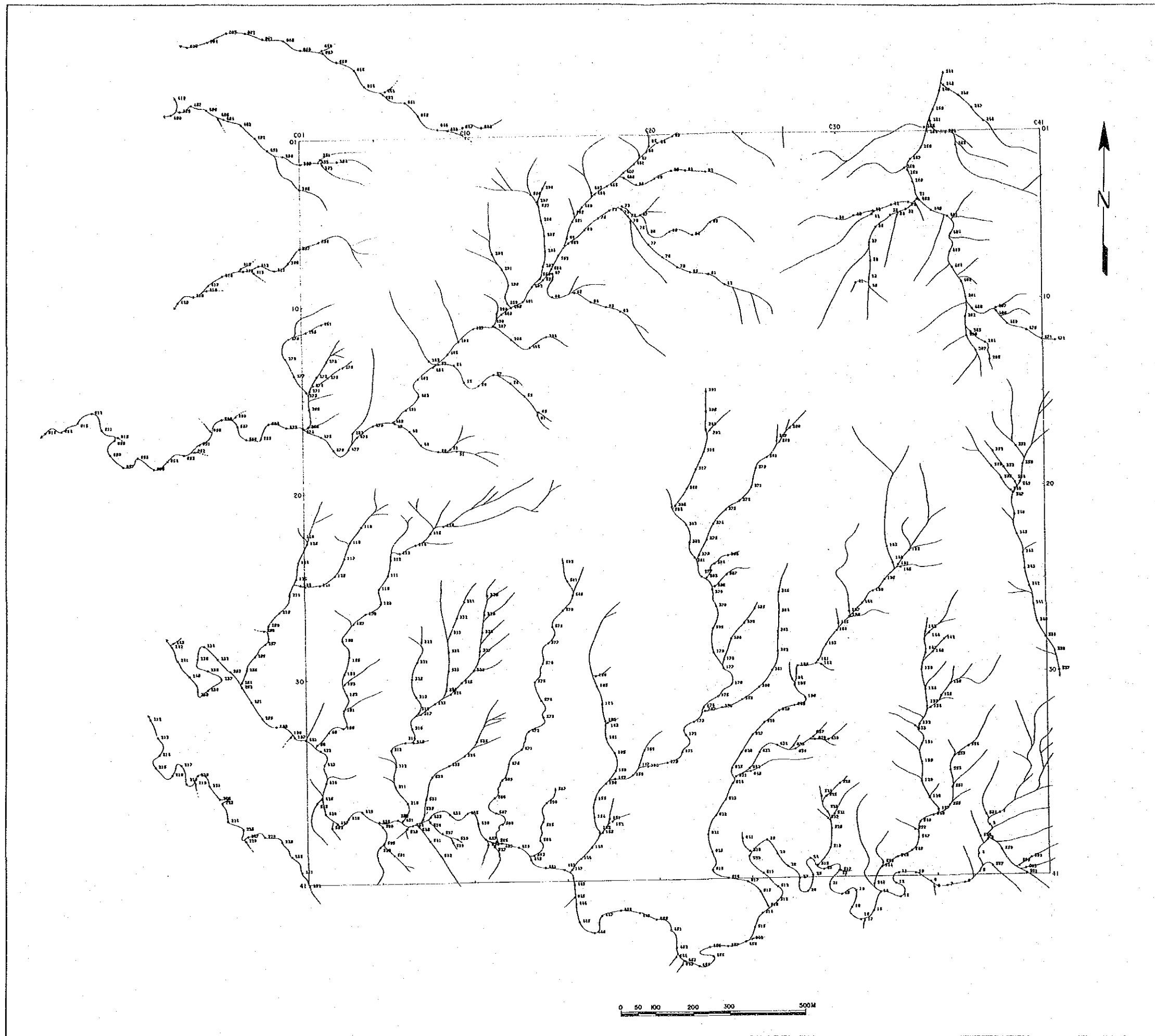


Fig. 93

Location Map of Stream Sediment Samples in "c" Area

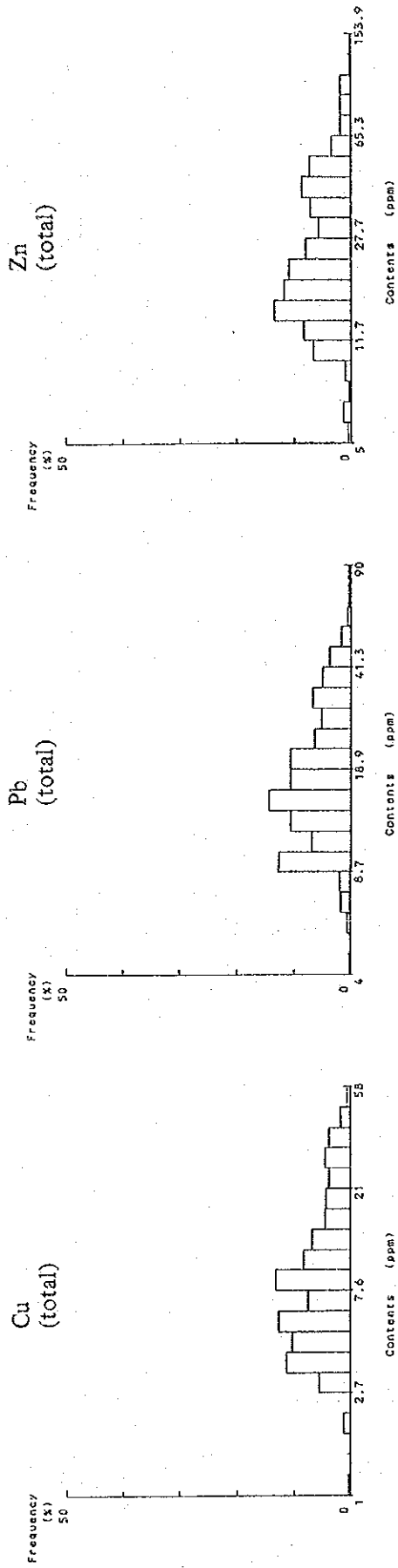


Fig. 94 Histogram for Stream Sediment Samples in "c" Area

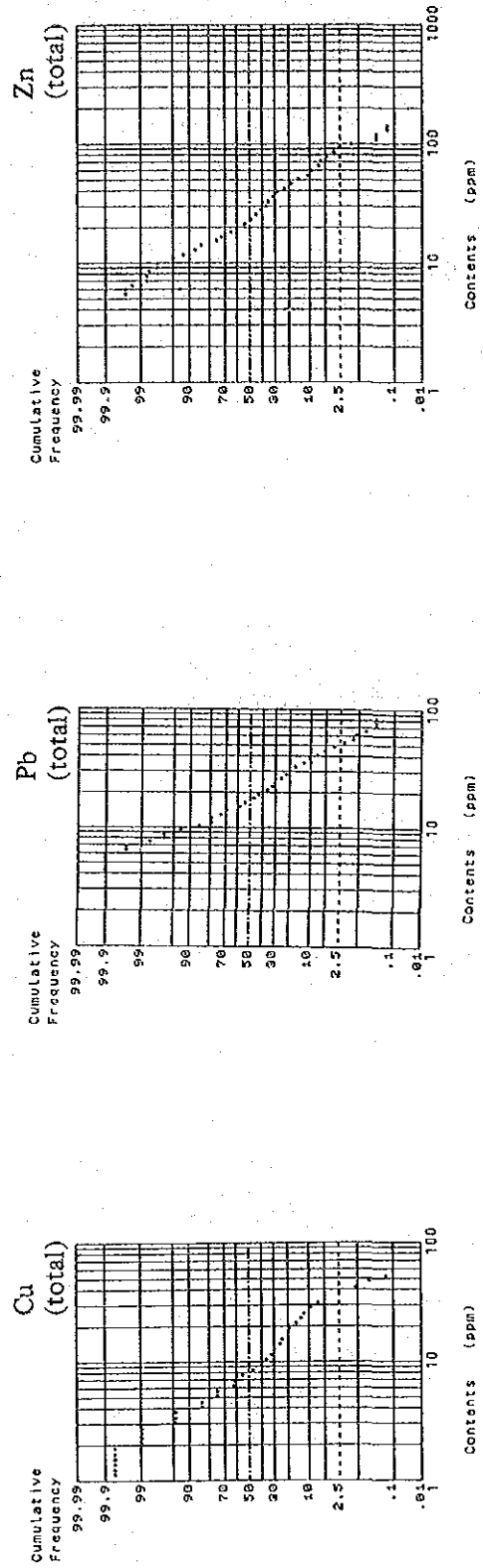


Fig. 95 Cumulative Frequency Curve for Stream Sediment Samples in "c" Area

Table 21 Statistic Values for Stream Sediment Samples in "c" Area

			Intrusive rock	Sedimentary rock	Total
Cu (ppm)	Number of samples	(n)	117	548	665
	Maximum value	(Vmax)	58	44	58
	Minimum value	(Vmin)	3	1	1
	Geometric mean	(\bar{X})	18.1	7.3	8.6
	Standard deviation	(t)	0.281	0.272	0.312
	$10^{\log \bar{x} + t}$		34.6	13.7	17.6
	$10^{\log \bar{x} + 2t}$		(66.0)	25.6	36.2
	$10^{\log \bar{x} + 3t}$		(126.1)	(47.8)	(74.2)
Pb (ppm)	Number of samples	(n)	117	548	665
	Maximum value	(Vmax)	71	90	90
	Minimum value	(Vmin)	4	6	4
	Geometric mean	(\bar{X})	22.2	16.7	17.6
	Standard deviation	(t)	0.223	0.218	0.224
	$10^{\log \bar{x} + t}$		37.1	27.6	29.5
	$10^{\log \bar{x} + 2t}$		62.0	45.6	49.4
	$10^{\log \bar{x} + 3t}$		(103.6)	75.3	82.7
Zn (ppm)	Number of samples	(n)	117	548	665
	Maximum value	(Vmax)	103	154	154
	Minimum value	(Vmin)	10	5	5
	Geometric mean	(\bar{X})	34.5	22.2	24.0
	Standard deviation	(t)	0.234	0.266	0.270
	$10^{\log \bar{x} + t}$		59.1	41.0	44.7
	$10^{\log \bar{x} + 2t}$		101.0	75.6	83.2
	$10^{\log \bar{x} + 3t}$		(173.7)	139.4	(154.9)
Mo (ppm)	Number of samples	(n)	117	548	665
All data show the values below detection limit.					

note) () ; value not present

Correlation Matrix

	Cu	Pb	Zn
Cu	1	-	-
Pb	0.551	1	-
Zn	0.574	0.834	1

In the upper reaches of a northerly trending creek in the central part of the area (sample Nos. 385 to 390 and 372 to 376).

The distribution is well consistent with that of Pb, and it is assumed that the correlation is high in reference to the values larger than $\bar{X} + 2t$.

(2) Result of Analysis by Score Sum

Fig. 96 (Map 78) shows the result of analysis by score sum.

Based on the distribution of the elements, the followings are recognized from score sum diagram.

The samples which have score 6 are No. 389 collected at the uppermost reaches of a northerly trending creek in the central part and No. 582 at the uppermost reaches of a north-northeasterly trending creek in the southwestern part area.

These are considered to be the zones of the highest potential in the survey area.

Next, the values larger than score 4 (containing at least one element which has the value larger than $\bar{X} + 2t$) will be discussed. The distribution is as follows.

In the intrusive rock in the northeastern part (sample Nos. 42 to 46).

In the branch of a northeasterly trending creek in the northwestern part (sample Nos. 66, 68, 74, 75, 79, 82 and 93).

In the uppermost reaches of a northerly trending creek in the central part (sample Nos. 386 to 389 and 372 to 374).

In the uppermost reaches of a north-northeasterly trending creek in the southwestern part (sample Nos. 578 and 582).

The distribution of these is quite similar to that of Pb and Zn made clear in the simple component analysis, and it is reflected by anomalies of these two elements.

When compared with the result of geologic mapping, the distribution of the high score values corresponds to the terrain of intrusive granodiorite porphyry in the northeastern part; in the northwestern part, to the area distributed by the small stock and the swarm of small dykes intruded into the sedimentary rock; in the central part, to the surrounding area of the stock located in the northeastern part and in the southwestern part, to the areas distributed by the dykes intruded into the sedimentary rocks. On the other hand, the distribution of the mineralized zones and alteration zones confirmed by the geologic mapping are found in most of the areas in the above, showing a very good consistency to each other.

2-2-5 Discussion

The result of the drainage survey will be compared with the result of soil geochemical survey.

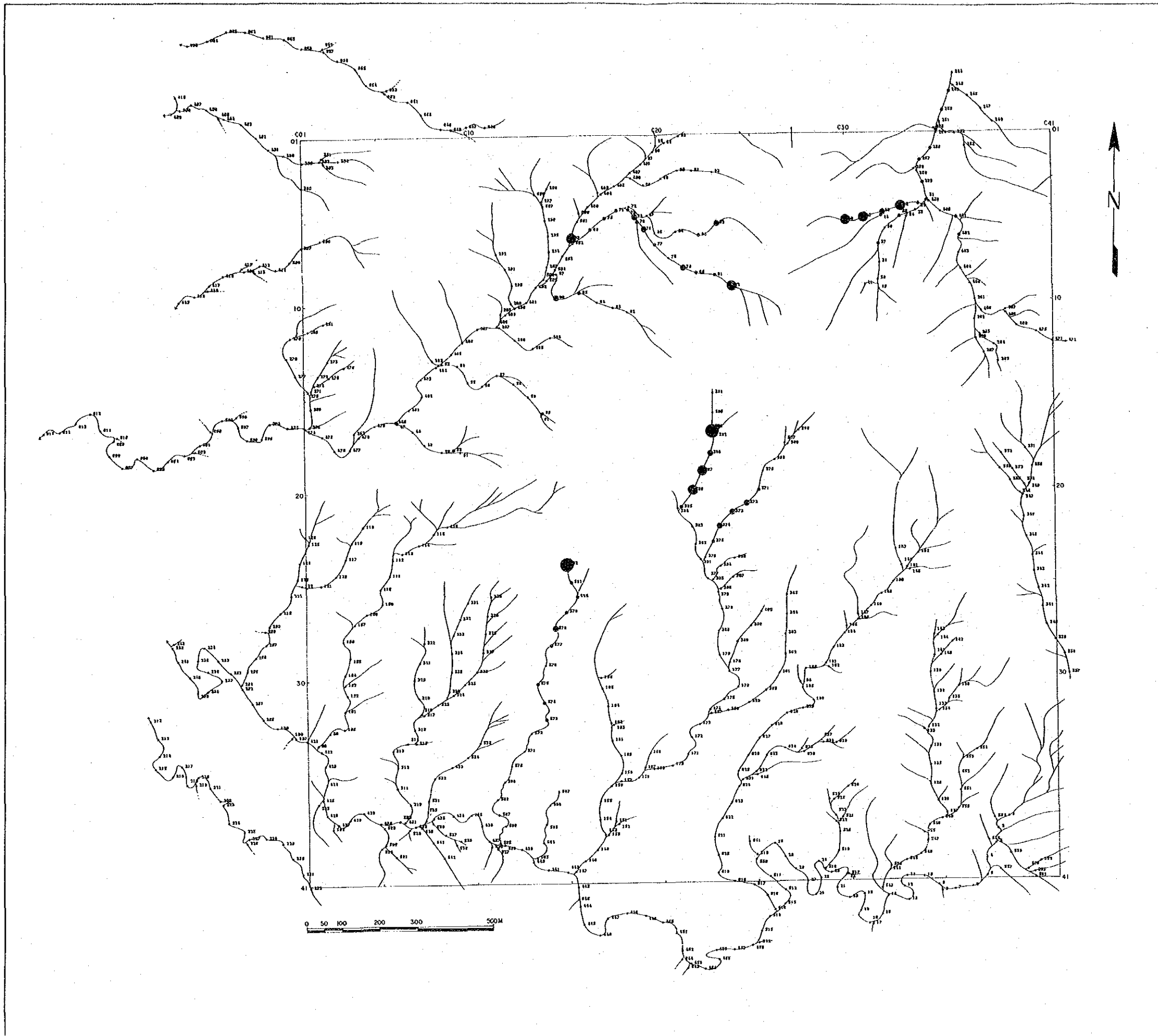
Four areas were extracted as the anomalous areas by the drainage survey, and these distribution show a very good consistency with the result of soil geochemical survey. The details are described in the following:

(1) The area of the highest potential found in the area is located in the uppermost reaches of a north-northeasterly trending creek in the southeastern part, which is consistent with the anomaly C15-21 detected by soil geochemical survey.

(2) The anomaly recognized in the eastern part of the area is consistent with the soil geochemical survey, which agrees with the distribution of mineralized silicification zones spread over the surrounding area of the stock of granodiorite porphyry in the northeastern part of the area.

(3) The result of the soil geochemical survey and that of the stream sediment show a discrepancy of about 100 meters in general. This seems to show the distance of move of the stream sediments transported by the stream.

(4) The correlation between Pb and Zn is high in the area, which was confirmed by the both geochemical surveys of soil and stream sediments.



LEGEND

- Score = 6
- Score = 5
- Score = 4
- Score = 3
- Score = 2
- sample location with serial number

Fig. 96
Score-Sum Map of Stream Sediment Samples in "c" Area

Chapter 3 Overall Discussion

For the survey of the first year, detailed geological mapping, geochemical surveys by soil and stream sediment were conducted in the c area.

The selection of this area was based on the following:

(1) Interpretation of Landsat imagery and aerial photographs on a scale of 1:500,000 and 1:25,000 shows the presence of "ring structures".

(2) The geological setting of the area is similar to the Mamut mine area.

(3) Pb, (Zn), (Cu) anomalies were detected in stream sediments which were collected during the UNDP survey in 1965 but subsequently reanalysed and reevaluated by the joint Malaysian-German Mineral Exploration Project in 1981.

The result of Phase I survey confirmed that the ring-shaped lineament is due to the intrusion of granodiorite porphyry which occurs over the northeastern to central parts of this area in the form of stocks and dykes.

In addition to this, the anomalies detected in stream sediments are caused by weak alteration and mineralization in sedimentary rocks surrounding the intrusive bodies of granodiorite.

As the result of this survey, it was concluded that:

(1) Geologically, the sedimentary rocks which are widely distributed in the area, show distinct characteristics of rock facies similar to those of the Crocker Formation rather than the Trusmadi Formation; however the regional geology surrounding the area was previously correlated to the Trusmadi Formation. Therefore, it is necessary to re-evaluate the regional and local geology.

(2) The distribution and scale of mineralization in the Area are rather local and weak, and thus less interesting for further exploration. However the mineralized zone, can be delineated as marginal to the main granodiorite, and is distributed as follows:

- bleached and altered zone bearing minor copper minerals around the eastern boundary of the area (and probably extending outside of area).
- small anomaly around the central part of the area (near the survey point of C15-21) which shows value of Cu : 383 ppm, Pb : 406 ppm, Zn : 282 ppm, Mo : 3 ppm and Au : 0.14 ppm in soils ; no in situ outcrop occurs as it is soil-covered.

PART V CONCLUSION AND RECOMMENDATION

1. Conclusion

From the results of geological, geochemical and geophysical (CSAMT, IP and SIP methods) surveys and drilling (MJM-1 ~ MJM-10 holes), the following conclusions are summarized:

(1) A, a (Bambangan) Area

(i) The geophysical survey using CSAMT method detected three anomalous resistivity zones (A-1, A-2, A-3) with 30–50 ohm-m. As A-1 anomalies with about 50 ohm-m underlying the Pinosuk Gravels was supposed to be related to the hydrothermal alteration.

IP and SIP surveys were carried out in the area and detected distinct IP anomalies on the west bank of the Bambangan Creek (near the survey points of 500W on line E and F).

The drilling hole (MJM-8) intersected the mineralized zone with chalcopyrite-pyrite dissemination of a porphyry copper type in the IP anomalous zone which is situated on the level of 120 m below the Bambangan Creek.

The estimated grade for the length of 83.80 m will be around 0.2 g/T Au, 0.4% Cu, 30 ppm Mo, whose better part of length of 20.60 m shows 0.7% of Cu.

From the point of the distribution of IP anomalies, the mineralized zone may extend in the direction of N-S.

(ii) As well as the result of MJM-8 hole, other drilling holes (MJM-2, 4, 6 and 7) intersected weak disseminated zone associated with the adamellite porphyry intrusion.

The altered minerals of tremolite and biotite found in each drilling hole, indicating the mineralization in serpentinite, whose grade of alteration has a tendency of strengthening westward.

Therefore, there may have a possibility indicating the center part of mineralization around MJM-2, 4 and 8.

(iii) It has become clear that the thickness of the Pinosuk Gravels is predominantly thicker than that was expected in the area between the Bambangan Creek and the Mamute mine. The bottom level of the Pinosuk Gravels rapidly deepens eastward from the Bambangan Creek, judging from the results of drilling. The thickness is 270 m at the location of drilling hole MJM-9. At the location of MUM-10, the thickness reaches more than 450 m, being reduced toward south.

(2) B, b (Mankadau) Area

(1) Geology and mineralization in this area seems to be closely related to the ophiolite sequence. The big floats of massive sulphide copper ore are recognized to be those from the ore deposit of a Cyprus type.

(2) Geological survey and geochemical survey by soil could not detect the outcrop of the ore

floats nor geochemical anomalies.

(3) CSAMT survey detected the low resistivity zone near the peridotite with high resistivity zone, suggesting strong argillization along faults.

(3) c (Paliu) Area

(1) The mineralization in this area, consisting of chalcopyrite – pyrite – pyrrhotite dissemination and arsenopyrite – (chalcopyrite) vein, is accompanied by granodiorite intrusions.

(2) Geological and geochemical surveys disclosed an alteration zone and geochemical anomalous zone for soil.

The former is a silicified zone with pyrite dissemination and extends toward outside of the surveyed area but no anomalies are associated. The latter is rather small, however it shows values of Cu: 383 ppm, Pb: 406 ppm and Zn: 282 ppm.

2. Recommendation for Phase II Survey

Based on the results of Phase I survey, the followings will be recommended for the next survey.

(1) Bambang Area

(i) Drilling to confirm the extension of the porphyry copper type mineralization which has been intersected by the drilling holes of MJM-2, 6 and 8 at the western bank of the Bambang Creek.

(ii) IP and SIP surveys in the A-3 low resistivity zone to find out a porphyry copper type mineralization, because the A-3 zone is considered to be caused by the hydrothermal alteration as well as the A-1 zone.

(2) Mankadau Area

Semidetailed geological and geochemical surveys to investigate the potential for massive copper sulphide and chrome-nickel ore deposits.

(3) Paliu Area

Trenching to clarify the sources of Cu, Pb and Zn geochemical anomalies detected in the central area.

REFERENCES

REFERENCES

- Fitch F. H. (1958) : The Geology and Mineral Resources of the Sandakan Area, North Borneo. Borneo Region, Malaysia Geological Survey Memoir 9, P115–152.
- Collenette P. (1958) : The Geology and Mineral Resources of the Jesselton–Kinabalu area. North Borneo Brit. Borneo Geol Survey Memoir 6, P1–194.
- Liechti P., Roe F. W. and Haile N. S. (1960) : The Geology of Sarawak, Brunei and the western part of North Borneo. Brit. Borneo Geol. Surv., Bull. 3, 360P.
- Walker P. B. et al. (1961) : Secondary Dispersion on Copper from the Karang Lode, North Borneo. Borneo Region, Malaysia Geological Survey Bull. 4, P91–118.
- Kirk H. J. C. (1963) : Igneous Rocks of North Borneo and Sarawaku Borneo Geol, Surv. Ann Report for 1962, P20–29.
- Kirk H. J. C. (1963) : Cinnabar near Rabau. North Borneo Geol, Surv. Ann Report for 1962 P155–157.
- Fitch F. H. (1958) : The Geology and Mineral Resources of the Sandakan Area, North Borneo. Region, Malaysia Geological Survey Memoir 9, P115–152.
- Collenette P. (1958) : The Geology and Mineral Resources of the Jesselton – Kinabalu area. North Borneo Brit. Borneo Geol Survey Memoir 6, P1–194.
- Liechti P., Roe F. W. and Haile N. S. (1960) : The Geology of Sarawak, Brunei and the western part of North Borneo. Brit. Borneo Geol. Surv., Bull. 3, P360.
- Walker P. B. et al. (1961) : Secondary Dispersion on Copper from the Karang Lode, North Borneo. Borneo Region, Malaysia Geological Survey Bull. 4, P91–118.
- Kirk H. J. C. (1963) : Igneous Rocks of North Borneo and Sarawaku Borneo Geol, Surv. Ann Report for 1962, P20–29.

- Kirk H. J. C. (1963) : Cinnabar near Rabau. North Borneo Geol, Surv. Ann Report for 1962, P155–157.
- Kirk H. J. C. (1964) : Igneous Rocks of North Borneo and Sarawaku Borneo Geol, Surv. Ann Report for 1962, P29–31, for 1963, P82–89.
- Cooper R. A., Woolf D. L. and Tooms J. S., (1964) : A geochemical reconnaissance survey of part of the Labuk Valley, Sabah Borneo Region Malaysia Geol Survey Ann Report for 1963, P176–185.
- Kirk H. J. C. (1964) : Igneous Rocks of North Borneo and Sarawak Borneo Geol, Surv. Ann Report for 1962, P31–36, for 1963, P89–94, P176–185.
- Collenette P. (1965) : The geology and mineral resources of Pensiangan and upper Kinabatangan area, Sabah, Malaysia. Borneo Reg. Malaysia Geol. Surv. Mem., 12, P1 ~ 150.
- Collenette P. (1965) : Prospecting in Sabah by Borneo Mining Limited 1959–1963. Borneo Reg., Malaysia Geol. Surv. Ann. Report for 1964, P57–61.
- Kirk H. J. C. (1965) : Igneous Rocks of North Borneo and Sarawak Borneo Reg., Malaysia Geol. Surv. Ann. Report for 1964, P87–91.
- Collenette P. (1965) : Geochemical Survey Labuk Area 1963–4, Borneo Reg., Malaysia Geol. Surv. Ann. Report for 1964, P50–51.
- Newton – Smith J. (1965) : The Bidu – Bidu Hills, Sabah (Report 4), Borneo Reg., Malaysia Geol. Surv. Ann. Report for 1964, P114–121.
- Lewis D. E. (1965) : Case History of a Geochemical Anomalous Copper Zone and Pinanduan, Sabah, Malaysia, Borneo Reg., Malaysia Geol. Surv. Ann Report for 1964, P163–175.
- Collenette P. (1965) : The geology and mineral resources of Pensiangan and upper Kinabatangan area, Sabah, Malaysia. Borneo Reg., Malaysia Geol. Surv. Mem. 12, P1 ~ 150.

- Newton – Smith J. (1966) : Geology and copper mineralization in the Mamut River area, Kinabalu. Borneo Reg., Malaysia Geol. Surv. Ann. Report for 1965, P40–68, 88–96.
- Woolf D. L., Tooms J. S. and Kirk H. J. C. (1966) : Geochemical Survey in the Labuk Valley, Sabah. Borneo Reg., Malaysia Geol. Surv. Ann. Report for 1965, P212–226.
- Kirk H. J. C. (1966) : The Mineralogy of Pinanduan Copper deposit, Sabah, Malaysia. Borneo Reg., Malaysia Geol. Surv. Ann. Report for 1965, P196–204.
- Winkler H. A. (1966) : Geophysical Prospecting in the Kinabalu and River Sualong Area, Labuk Valley, Sabah. Borneo Reg., Malaysia Geol. Surv. Ann. Report for 1965, P205–211.
- Wilford G. E. (1967) : Geological map of Sabah, East Malaysia, 2nd ed., Borneo Reg., Malaysia Geol. Surv.
- Wong N. P. Y. (1967) : Geology and copper mineralization of the Bambang valley, Kinabalu, Sabah. Borneo Reg., Malaysia Geol. Surv. Bull. 8, P81–88.
- Stauffer P. H. (1967) : Studies in the Crocker Formation, Sabah, Borneo Reg., Malaysia Geol. Surv., Papers 1966, Bull 8, P1–13.
- Wong N. P. Y. (1967) : Geology and copper mineralization of the Bambang valley, Kinabalu, Sabah. Borneo Reg., Malaysia Geol. Surv., Geol. Papers 1966, Bull. 8, P81–88.
- Koopmans B. N. and Stauffer P. H. (1967) : Glacial Phenomena on Mount Kinabalu, Sabah. Borneo Reg., Malaysia Geol. Surv., Geol. Papers 1966, Bull 8, P25–35.
- Kirk H. J. C. (1966) : Hydrothermal mineralization and igneous rocks in East Malaysia. Borneo Reg., Malaysia Geol. Surv., Geol. Papers. Bull 8, P53–61, 1967
- Kirk H. J. C. (1967) : The Mamut Copper Prospect, Kinabalu, Sabah Borneo Reg., Malaysia Geol. Surv., Geol. Papers 1966, Bull 8, P68–80.

- Collenette P. (1967) : Labuk Valley, Mineral Investigation and Consequent Development, Borneo Reg., Malaysia Geol. Surv. Ann. Report for 1966, P68–71.
- Kirk H. J. C. (1967) : Diamond Drilling Costs at the Mamut Prospect, Kinabalu, Kinabalu, Sabah, Borneo Reg., Malaysia Geol. Surv. Ann. Report for 1966.
- Kirk H. J. C. (1967) : Porphyry Copper Deposit in Northern Sabah, Malaysia Trns. Instn. Mining Metal (Section B : Appl. Earth Sci) Vol. 6. PB212–3.
- Newton – Smith J. (1967) : Bidu – Bidu Hills Area, Sabah, East Malaysia Borneo Reg., Malaysia Geol. Surv. Report 4.
- Lewis D. E. (1967) : The Karang Copper Prospect, Karamuak Valley, Sabah Malaysia Borneo Reg., Malaysia Geol. Surv., Geol. Papers Bull 8, P62–67.
- Wong N. P. Y. (1967) : Mount Silam Area, Sabah (Report 7) Borneo Reg., Malaysia Geol. Surv. Ann. Report for 1966, P62–68.
- Stauffer P. H. (1968) : Glaciation of Mount Kinabalu Geol. Soc. Malaysia, Bull 1, P63.
- Wilfred G. E. (1968) : Notes on the geomorphology of Sabah, Borneo Reg., Malaysia Geol. Surv., Geol. Papers 1967, Bull 9, P1–22.
- Wilfred G. E. (1968) : Iron and Nickel prospecting at Tavai Plateau 1962–64, Sabah Borneo Reg., Malaysia Geol. Surv., Geol. Papers 1967, Bull 9, P80–87.
- Haile N. S. (1968) : The northwest Borneo geosyncline in its geotectonic setting. Geol. Soc. Malaysia Bull. 1, P59.
- Hutchison C. S. (1968) : Tectogene hypothesis applied to the pre-tertiary of Sabah and the Philippines Geol. Soc. Malaysia Bull. 1, P65–79.
- Wong N. P. Y. (1968) : Segama – Darvel Bay Area, Borneo Reg., Malaysia Geol. Surv. Ann. Report for 1967, P48–52.

- Wong N. P. Y. (1968) : Geochemical Prospecting, Segama Area. Borneo Reg., Malaysia Geol. Surv. Ann. Report for 1967.
- G. S. (1968) : Geochemical Prospecting in the Semporna Peninsula, Borneo Reg., Malaysia Geol. Surv. Ann. Report for 1967, P66–70.
- Haile N. S. (1969) : Geosynclinal theory and the organizational pattern of the northwest Borneo geosyncline. Geol. Soc. London Quart. Jour., 124, P171–194.
- Kasama T., Akimoto H., Sada S. and Jacobson G. (1970) : Geology of the Mt. Kinabalu area, Sabah, Malaysia Jour. Geoscience, Osaka City Univ., 13 (6), P113–148.
- Jacobson G. (1970) : Gunong Kinabalu area, Sabah, Malaysia. Geol. Surv. Malaysia Reprot, 8, P1–111.
- Leong T. K. (1970) : Bouldery mudflow deposit at Ranau, Sabah, East Malaysia. Geol. Soc. Malaysia Bull. 3, P139–146.
- Leong Khee Meng (1970) : Introduction to the Geology of the Ranau – Paranchangan Area, Sabah, Malaysia Geol. Surv. Ann. Report, P148–150.
- Leong Khee Meng (1972) : Ranau – Paranchangan Area. (Report 12). Malaysia Geol. Surv. Ann. Report.
- Jacobson G. and Kim P. (1972) : Some engineering properties of Sabah rocks. Malaysia Geol. Surv., Geol. Papers, Vol. 1, P18–27.
- Lim P. S. (1974) : Geology and copper mineralization of the Mamut area, Sabah, East Malaysia. B. Sc. thesis, Univ. Malaya, P1–117.
- Stauffer P. H. (1974) : Malaya and Southeast Asia in the pattern of continental drift. Geol. Soc. Malaysia Bull. 7, P89–138.

- Tokuyama A. and Yoshida S. (1974) : Kinabalu Fault, a large strike-slip fault in Sabah, East Malaysia. In *Geology and palaeontology of southeast Asia* (Kobayashi T. and Toriyama R. eds) Univ. Tokyo Press. 14, P175–188.
- Hutchison C. S. (1975) : Ophiolites in Southeast Asia. *Geol. Soc. Am. Bull.* 86, P797–806.
- Creasey S. C. (1977) : Intrusives associated with porphyry copper deposits. *Geol. Soc. Malaysia Bull.* 9, P51–66.
- Leong K. M. (1977) : New ages from radiolarian cherts of the Chert–Spillite Formation, Sabah. *Geol. Soc. Malaysia Bull.* 8, P109–111.
- Myers L. C. (1977) : A weathering profile developed on ultrabasic rocks at Telupid, Sabah. *Malaysia Geol. Surv., Geol. Papers Vol. 2*, P66–71.
- Nagano K., Takenouchi S., Imai H. and Shoji T. (1977) : Fluid inclusion study of the Mamut porphyry copper deposit, *Mining Geology (Japan) Vol. 27*, P201–212.
- Shoji T., Imai H. and Takenouchi S. (1977) : Study on microprobe microanalysis of the ore minerals from the Mamut mine, Sabah, Malaysia. *Mining Geology (Japan) Vol. 27*, P323–330.
- Newton – Smith J. (1977) : Geology and mineralization at the Mamut Copper Prospect, Sabah. *Malaysia Geol. Surv., Geol. Papers Vol. 2*, P55–65.
- Singh D. S. and Khoo T. T. (1977) : A review of the progress in knowledge of the geology and mineral resources of Malaysia from 1972 to early 1975. *Geol. Soc. Malaysia Bull.* 8, P95–107.
- Hutchison C.S. (1978) : Ophiolites metamorphism in northeast Borneo. *Lithos* 11, P195–208.
- Titley S. R. (1978) : Copper, molybdenum, and gold content of some porphyry copper systems of the southwestern and western Pacific. *Econ. Geol.* 73, P977–981.
- Chung S. K. (1978) : Geological Survey of Malaysia, Ann Report for 1978. *Malaysia Geol. Surv.*, P67–77, P95–109.

- Kosaka H. and Wakita K. (1978) : Some geologic features of the Mamut porphyry copper deposit. *Econ. Geol.* 73, P618–627.
- Lee D. (Chung S. K.) (1979) : Geological Survey of Malaysia Ann. Report for 1979, Copper. *Malaysia Geol. Surv.* P68–79, P119–129.
- Bol, A. J. and Hoorn, B. (1980) : Structural styles in Western Sabah offshore. *Geol. Soc. Malaysia, Bull.* 12, P1–16.
- O. M. R. D. Sabah (1981) : Introducing Mamut Copper Mine, Sabah, *Malaysia Sarawak Mining Industries Ass. Vol. 1*, P59–61.
- Lim P. S. (1982) : Geology of the Mankadau area, Merungin. *Geol. Surv. of Malaysia Ann. Report*, P251–254.
- Nishiyama T. (1983) : Minor elements in pyrite and chalcopyrite from the Mamut mine, Malaysia. *Mining Geol. (Japan)* 33, P1–7.
- Walker P. B. (1961) : Report on Geochemical Surveys in Karang and Tambuyukon Concession. *GSJL 007/61* (Unpublished).
- Hillebrand J. R. (1962) : First quarter progress report Borneo Exploration Programme, *GSJL 007/62* (Unpublished).
- Hillebrand J. R. (1963) : Report on Investigation of the Mankadau Mineral District, West Coast Residency, North Borneo, *GSJL 007/65* (Unpublished).
- Woolf D. L. (1965) : Report on the Labuk Valley Natural Resources Survey : Geochemical Investigations 1963–1965. *GSJL 210/13 P80* (Unpublished).
- Kirk H. J. C. (1968) : The igneous rocks of Sabah and Sarawak, Borneo Reg., *Malaysia Geol. Surv. Bull.* 5, P201 Kuching.

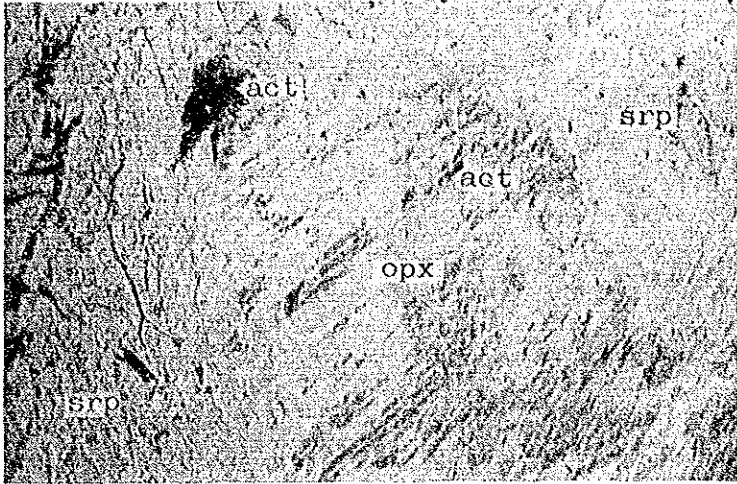
- Leong T. K. (1969) : Clastic Sediments and Sedimentary rocks of the Ranau area, Sabah, East Malaysia. B. Sc. (Hons) thesis, University of Malaya Kuala Lumpur (Unpubl.).
- Bull P. F. (1976) : The Gunung Nungkok Copper Prospect. M. Sc thesis, University of London (Unpubl.).
- Hoppe P., Weber H. S. & Yan A. (1981) : Geochemical prospecting in Kinabalu – Ranau Paranchangan area, M. G. M. & J. K. B. S. 81/4.
- Hoppe P. (1982) : Report on photogeology of the Paranchangan Sungai Paliu Area. M. G. M. & J. K. B. S. 82/2.
- Hoppe P. (1982) : Report on field check in Sungai Paliu Area, M. G. M. & J. K. B. S. 82/4 (Unpublished).
- Akiyama Y. (1984) : A case history – exploration, evaluation and development of the Mamut porphyry copper deposit, Geol. Soc. Malaysia., Bull. 17 P. 237–255.
- MMAJ (1970) : Aeromagnetic Survey of the Kinabalu – Tambuyukon Area, Saba, Malaysia. Hunting Geology and Geophysics Ltd.
- Leong K. M. (1974) : The Geology and Mineral Resources of the upper Segama Valley and Darvel Bay Area Sabah, Malaysia Geol. Sur. Memoir 4.

APPENDICES

A-1 Microphotograph of Thin Sections

Abbreviation

q	: quartz
kf	: k-feldspar
pl	: plagioclase
bi	: biotite
hb	: hornblende
au	: augite
opx	: orthopyroxene
cpx	: clinopyroxene
ol	: olivine
chr	: chromite
gl	: glass
cal	: calcite
ser	: sericite
chl	: chlorite
srp	: serpentine
act	: actinolite
zeo	: zeolite
ht	: hematite
op	: opaque mineral
()	: pseudomorph



Only lower polar



Crossed polars

0 1.0 mm

Sample No. : S-31
Location : B07-10 ("b" Area)
Rock name : harzburgite